

Representation of the Visual Field in the Second Visual Area in the *Cebus* Monkey

MARCELLO G.P. ROSA, AGLAI P.B. SOUSA, AND RICARDO GATTASS
Instituto de Biofísica Carlos Chagas Filho, Universidade Federal do Rio de Janeiro,
RJ., 21.941, Brasil

ABSTRACT

The representation of the visual field in the second visual area (V2) was reconstructed from multiunit visual responses and anatomical tracers. Receptive field plotting was performed during multiple recording sessions in seven *Cebus apella* monkeys under N₂O/O₂ and immobilized with pancuronium bromide. V2 forms a continuous belt of variable width around striate cortex (V1) except at the most anterior portion of the calcarine sulcus. In each hemisphere V2 contains a visuotopic representation of the contralateral visual hemifield. The representation of the vertical meridian is adjacent to that of V1 and forms the posterior border of V2. The representation of the fovea of V2 is adjacent to that of V1. The representation of the horizontal meridian (HM) is continuous with that of V1; then it splits to form the anterior border of V2, both dorsally and ventrally. The lower quadrant of the visual field is represented dorsally and the upper quadrant ventrally. The visual topography of V2 is coarser than that of V1. In V2, receptive fields corresponding to recording sites separated by a cortical distance of up to 4 mm may represent the same portion of the visual field.

In three additional animals, combined injections of fluorescent tracers along the HM representation in V1 yielded two projection sites at the anterior border of V2. The split of the HM representation is estimated to occur at an eccentricity below 1°.

Quantitative analysis showed that in V2 the representation of the central visual field is magnified relative to that of the periphery. The cortical magnification factor is greater along the isopolar dimension than along the isoeccentric one. Receptive field size in V2 increases with increasing eccentricity.

In sections stained for myelin by the Heidenhein-Wöelcke method V2 can be distinguished from the surrounding cortex for most of its extent.

Key words: prestriate cortex, visuotopic organization, cortical magnification, receptive field size, New World monkey

Cowey, in 1964, described a partial representation of the visual field in the prestriate cortex adjacent to V1 in the squirrel monkey (*Saimiri*). Later, Allman and Kaas ('74) mapped a complete representation of the visual field in the comparable area of another New World monkey, the nocturnal owl monkey (*Aotus*). In Old World monkeys the presence of V2 was first suggested by Zeki ('69). Subsequently, Van Essen and Zeki ('78) mapped, in the macaque, the area of representation of the central 10° of the lower visual field in V2. Later, Gattass et al. ('81) defined the boundaries of V2 and studied its topographic organization. These authors have shown that V2, as defined by multiunit recordings, is coextensive with the area adjacent to V1 which receives

topographically organized projections from it (Cragg, '69; Zeki and Sandeman, '76; Rockland and Pandya, '81; Weller and Kaas, '83; Van Essen et al., '86).

The representation of the visual field in V2 was shown to be discontinuous at the representation of the horizontal meridian both in the macaque and in the owl monkey. This type of representation has been referred to as a "second order transformation of the visual hemifield" by Allman and Kaas ('74). The topographic organization of V2 in the owl monkey is slightly different from that found in the

Accepted February 22, 1988.

Abbreviations

Ca	calcarine sulcus
Ci	cingulate sulcus
Co	collateral sulcus
CMF	cortical magnification factor
HM	horizontal meridian
IO	inferior occipital sulcus
IP	intraparietal sulcus
La	lateral sulcus
Lu	lunate sulcus
OT	occipito temporal sulcus
Pa	paraoccipital sulcus
PO	parieto occipital cleft
POm	medial parieto-occipital sulcus
PRO	area prostriata
RF	receptive field
ST	superior temporal sulcus
VM	vertical meridian
V1	primary visual area
V2	second visual area

macaque, both in the relative emphasis of central vision representation and in the eccentricity at which the split of the horizontal meridian occurs. These differences may be related either to the visual habits and sizes of these monkeys or may represent a fundamental difference in the organization of the visual cortex of New World and Old World monkeys. In order to evaluate these hypotheses, we studied the visuotopic organization of V2 in *Cebus apella*, a New World monkey with diurnal habits, size and sulcal pattern similar to those of the Old World monkey *Macaca fascicularis*.

On the basis of recordings from small groups of neurons and the position of retrogradely labelled cells after injections of fluorescent tracers in V1, we report on the visual topography of V2 in the *Cebus*. Preliminary results have been previously described (Gattass et al., '84; Rosa et al., '84; Sousa et al., '86).

MATERIALS AND METHODS

Ten *Cebus apella* monkeys weighing between 2.2 and 4.0 kg were used: seven for electrophysiological mapping and three for anatomical tracing experiments.

A detailed description of the preanesthetic medication, induction and maintenance of anesthesia, immobilization, and electrode characteristics has been given elsewhere (Gattass and Gross, '81; Gattass et al., '87). Briefly, prior to the first recording session the animal was anesthetized (ketamine, 50 mg/kg and benzodiazepine, 2 mg/kg), and a stainless-steel well (35 mm in diameter) and a bolt for holding the animal in a stereotaxic apparatus were implanted under aseptic conditions. Supplementary doses of anesthetic were given when necessary. During the recording sessions, the animals were maintained under 70% nitrous oxide and 30% oxygen and immobilized with pancuronium bromide. The procedures concerning the eyes and the visual stimuli were also described in the same publications (Gattass and Gross, '81; Gattass et al., '87).

Electrophysiological mapping experiments

Four to six recording sessions were conducted for each of the seven animals used for electrophysiological mapping. These animals were systematically studied with vertical or oblique electrode penetrations (tilted posteriorly 20° in the parasagittal plane) carried out over a 4-week period. In each penetration recording sites were separated by 400–

500 μm . The topography of the visual field representation was established by relating the coordinates of the receptive fields of small clusters of neurons with the locations of the corresponding recording sites in V2.

The positions of the blind spot and of the fovea were projected onto a hemisphere by means of a reversible ophthalmoscope. During the recording session the position of the fovea was constantly monitored by means of a second electrode placed at the region of representation of the fovea in V1 (Gattass et al., '87).

Histology

The histological procedures were described in detail previously (Gattass and Gross, '81). Electrolytic lesions were made at several sites along each penetration. Alternate 40- μm frozen sections, either coronal or parasagittal, were stained for cell bodies with cresyl violet or for myelin with either a modified Heidenhein-Wöelcke stain (Gattass et al., '81) or with the Gallyas method ('79).

Anatomical tracing experiments

In three animals, after mapping the opercular surface of V1 with vertical penetrations 1.5 mm apart, the dura mater was opened and reflected to allow the injection of fluorescent tracers. The injection sites were then programmed, taking into account the magnification factors of V1 at the given eccentricity and the direct visualization of the anterior border of V1. This border is easily determined because in the *Cebus*, as in the squirrel monkey (Cowey, '64), V1 has a richer pattern of blood vessels than the surrounding cortex.

In each animal, 1 μl of a 2% solution of Nuclear Yellow (NY) in 0.9% saline and 1 μl of a 5% solution of bisbenzimidazole (BB) in 0.9% saline were injected by brief pulses of pressure on tapered glass micropipettes (40–70 μm) at two different eccentricities along the horizontal meridian representation in V1. The injections were made 600–800 μm from the cortical surface. After the injection the dura was sutured and the animal allowed to recover.

After 48 hours of survival the animal was deeply anesthetized with sodium pentobarbital (30 mg/kg) and perfused through the aorta with saline 0.9% followed by increasing concentrations of sucrose (10, 20, and 30%) in formaldehyde 4%. The brain was then removed from the skull, blocked and stored overnight in the refrigerator in formaldehyde 4%/sucrose 30%. It was then quickly frozen and sectioned (40 μm) either in the coronal or in the parasagittal plane. Nonstained sections were mounted in saline 0.5%, quickly dried, dehydrated, defatted, and coverslipped with Eukitt. Alternate sections were either stained for cells with cresyl violet or for myelin by the Gallyas ('79) method. The sections were analyzed under phase contrast and fluorescence techniques in a Zeiss Jena NU-2 microscope, with transmitted excitation light peaking at 366 nm (light source: HBO 200; filters: excitation, BG12 + UG1; barrier, OG1 or GG9). The sections were scanned under $\times 250$ magnification and plotted with the aid of an x-y plotter coupled to the microscope stage. The fluorescent dyes were identified by their hue and by their location in the cell body.

Two-dimensional maps

In order to obtain maps of the visual topography of V2 for each animal, we unfolded the relevant portions of extrastriate cortex by building three-dimensional models of layer IV

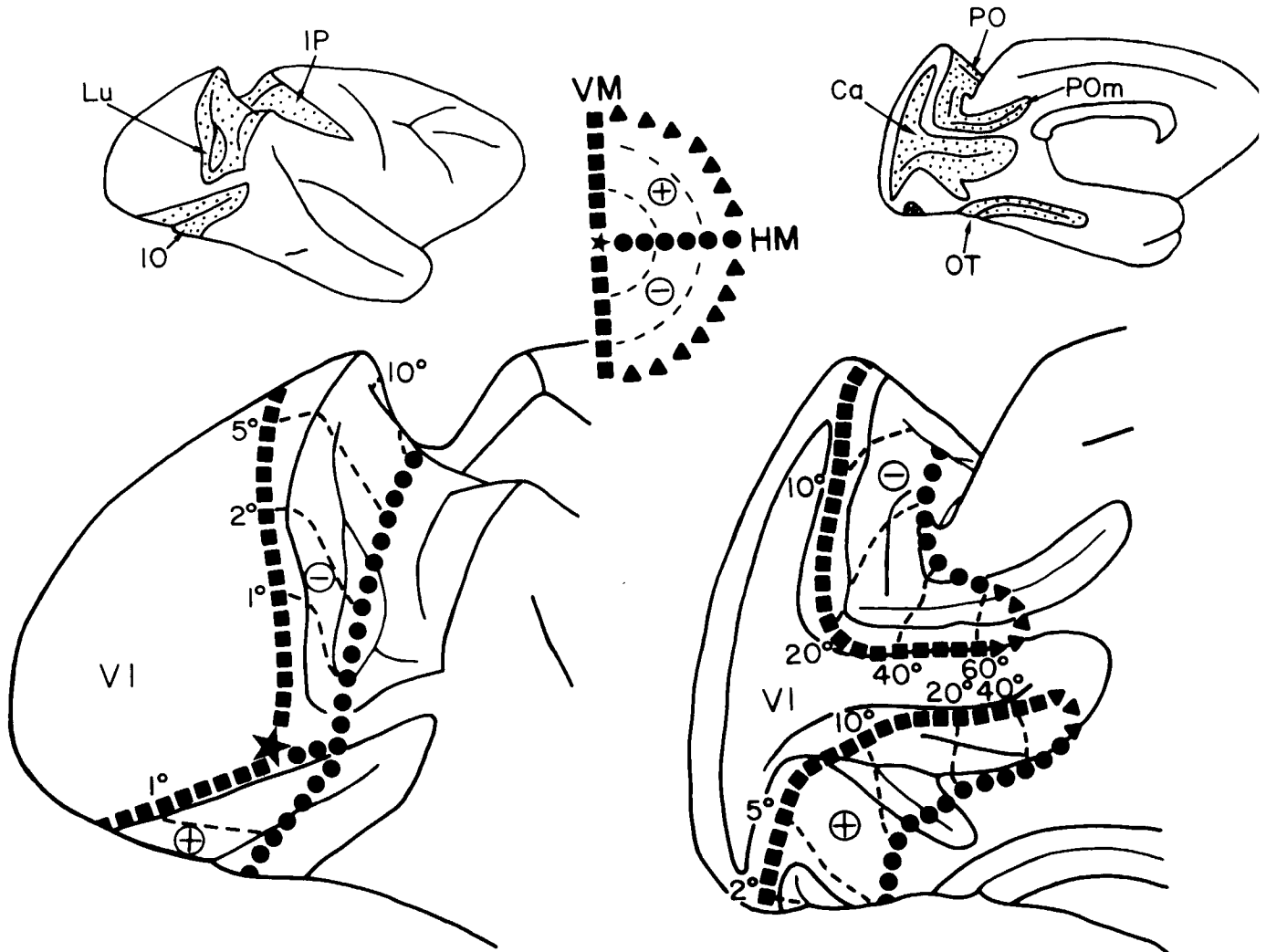


Fig. 1. Visuotopic organization of V2. The drawings are based on photographs of a brain in which sulci were partially opened (stippled areas in upper drawings). The squares indicate the vertical meridian (VM), the filled circles the horizontal meridian (HM), the triangles the periphery, and the

star the center of gaze. The dashed lines are isoeccentricity lines. Left drawings are lateral views and the right ones medial views. Inset is a representation of the visual hemifield in polar coordinates.

at $\times 7.5$ magnification and then unfolding them, following a procedure previously described (Gattass et al., '87). In reconstructing limited portions of V2, the "pencil and paper" technique with the controls described by Van Essen and Maunsell ('80) was used. An example of such a map is presented in Figure 8.

RESULTS

Throughout this paper the portion of V2 dorsal to the calcarine sulcus adjacent to the representation of the lower quadrant in V1 is referred to as "dorsal V2." Likewise, "ventral V2" refers to the part of V2 ventral to the calcarine sulcus adjacent to the upper quadrant representation in V1.

Location and overall organization

V2 forms a continuous belt around striate cortex except for a small gap at the anteriormost portion of the calcarine sulcus. V2 is widest (8–11 mm) close to the representation of 10° eccentricity and shows a constriction (4–5 mm) at the

region of foveal representation (Figs. 1, 4A). The area of V2 estimated on three-dimensional models in two animals was found to be 819 and 883 mm^2 . In these animals the area of V1 was found to be 1,049 and 1,115 mm^2 , respectively.

V2 contains a topographically organized representation of the contralateral visual hemifield, with virtually no invasion of the ipsilateral visual hemifield (Figs. 1, 6). The vertical meridian is represented along the V1/V2 border. The representation of the horizontal meridian in V2 splits and forms most of its border with other anteriorly located prestriate areas. The foveal representation in V2 is located laterally, adjacent to that of V1. The lower quadrant of the visual field is represented dorsally and the upper quadrant ventrally.

In V2 as in V1 (Gattass et al., '87) the representation of the central visual field is greatly magnified relative to that of the periphery so that more than half of its surface is dedicated to the representation of the central 10° .

Visuotopic organization of V2

Figure 2 illustrates the locations of receptive field centers and corresponding recording sites in V2 in a series of para-

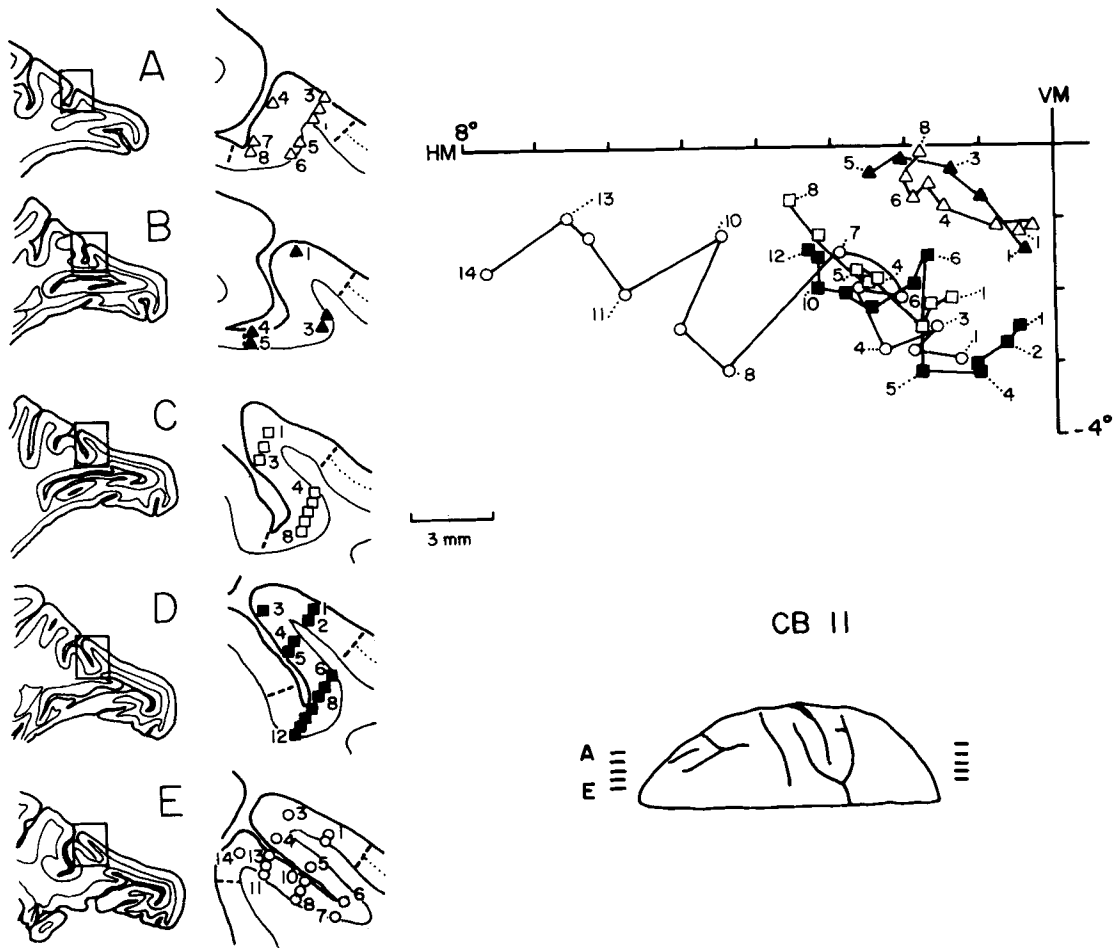


Fig. 2. Location of receptive field centers (right) corresponding to recording sites in dorsal (a, b) and ventral (c) V2. Sites are indicated in the parasagittal sections (A-G) cut at the levels indicated on the dorsal (inset in a,b) and ventral (inset in c) views of the brain. In 2c the region of

representation of the central visual field (inside the dashed box) is magnified in the lower right. The dashed lines on the sections indicate myeloarchitectonic borders of V2 and the dotted lines indicate layer IV in V1.

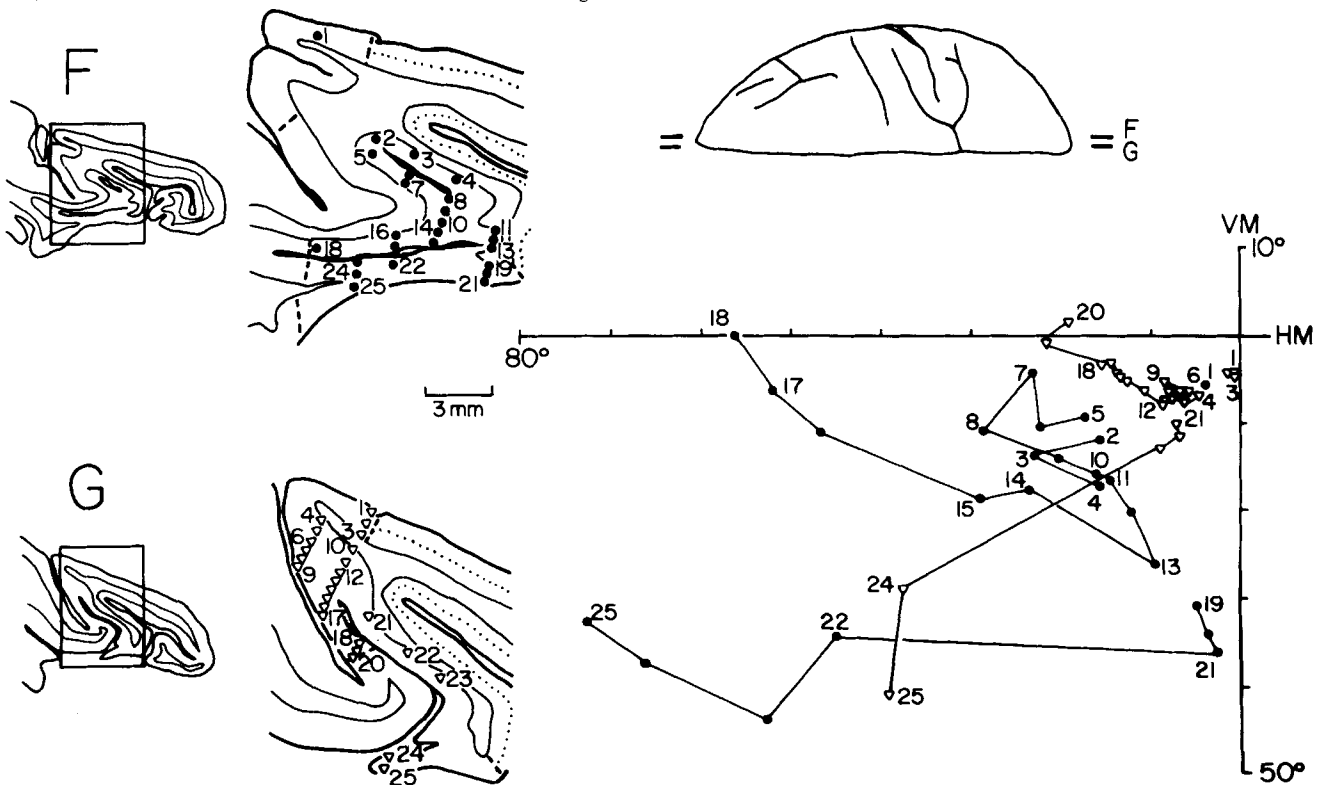


Figure 2b

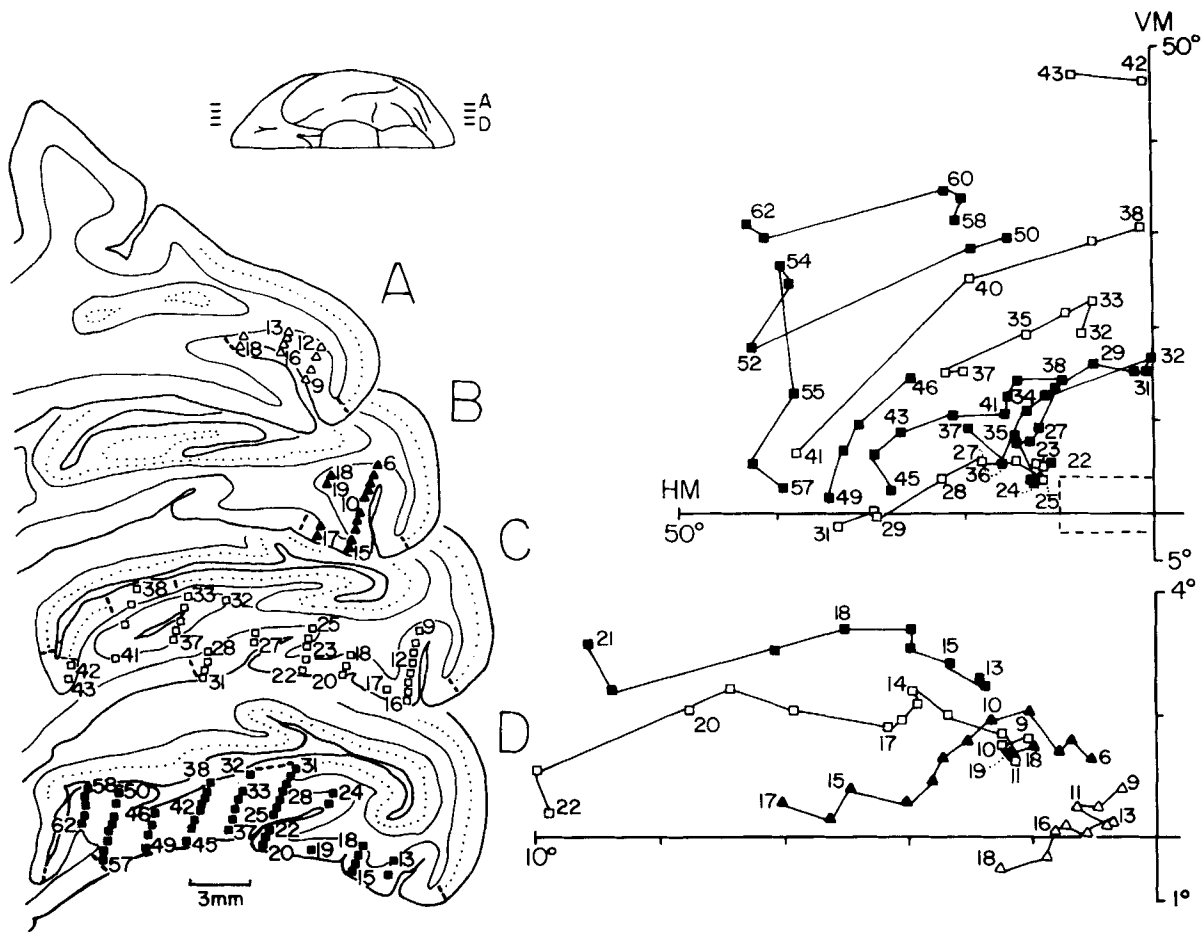


Figure 2c

sagittal planes spaced 2 mm apart in one animal. Sites located in dorsal V2 (Fig. 2a,b) correspond to receptive fields in the lower visual quadrant, while sites in ventral V2 (Fig. 2c) correspond to receptive fields in the upper visual quadrant. Receptive field centers corresponding to sites located close to the V1/V2 border are near the vertical meridian (for example, sites G1-3 in the lower visual field and sites D31 and D32 in the upper visual field). On the other hand, sites located close to the border of V2 with other prestriate areas are near the horizontal meridian (for example, sites A8 and F18). Note, however, that the centers of receptive fields corresponding to sites located at the anterior border of both dorsal and ventral V2 are not always coincident with the horizontal meridian; they occasionally invade the opposite visual quadrant.

In dorsal V2, recording sites on the lateral surface and lunate sulcus correspond to central receptive fields (Fig. 2a), whereas sites on the parietooccipital cleft, medial surface, and medial parietooccipital sulcus correspond to peripheral receptive fields (Fig. 2b). In ventral V2 recording sites located in the inferior occipital sulcus correspond to centrally located receptive fields (Fig. 2c, for example, sites A9-18). As one moves anteriorly along the tentorial surface across the collateral sulcus and along the lower bank of the calcarine sulcus there is an increase in receptive field eccentricity (see, for example, sites C17-31 and D15-62).

Figure 3 illustrates the location of receptive field centers and corresponding recording sites in a series of coronal sections from another animal. The visuotopic organization of V2 reconstructed from coronal sections is consistent with the above description. Note in this figure that the border between V1 and V2 represents the vertical meridian except for the anteriormost part of the calcarine sulcus, where recording sites close to this border correspond to the representation of the visual field periphery (sites F8-12; see also Fig. 8).

Inasmuch as V2 occupies several gyri and sulci in the occipital cortex, it is difficult to analyze the details of its visual topography in data presented in serial sections. Therefore, in order to obtain an overall view of the visual topography of V2, we projected the recording sites onto two-dimensional maps of the relevant portions of prestriate cortex.

Figure 4A illustrates an unfolded view of the striate and prestriate cortices corresponding to the hemisphere illustrated in Figure 2. The hatched region corresponds to V2. In order to minimize areal and angular distortions in V2 we introduced a discontinuity along the border of V1 and through area prostriata, as suggested by Van Essen et al. ('82). Figure 4B shows an enlarged view of the flattened model of V2 with the contours of layer IV of the sections used to build the model and the recording sites indicated

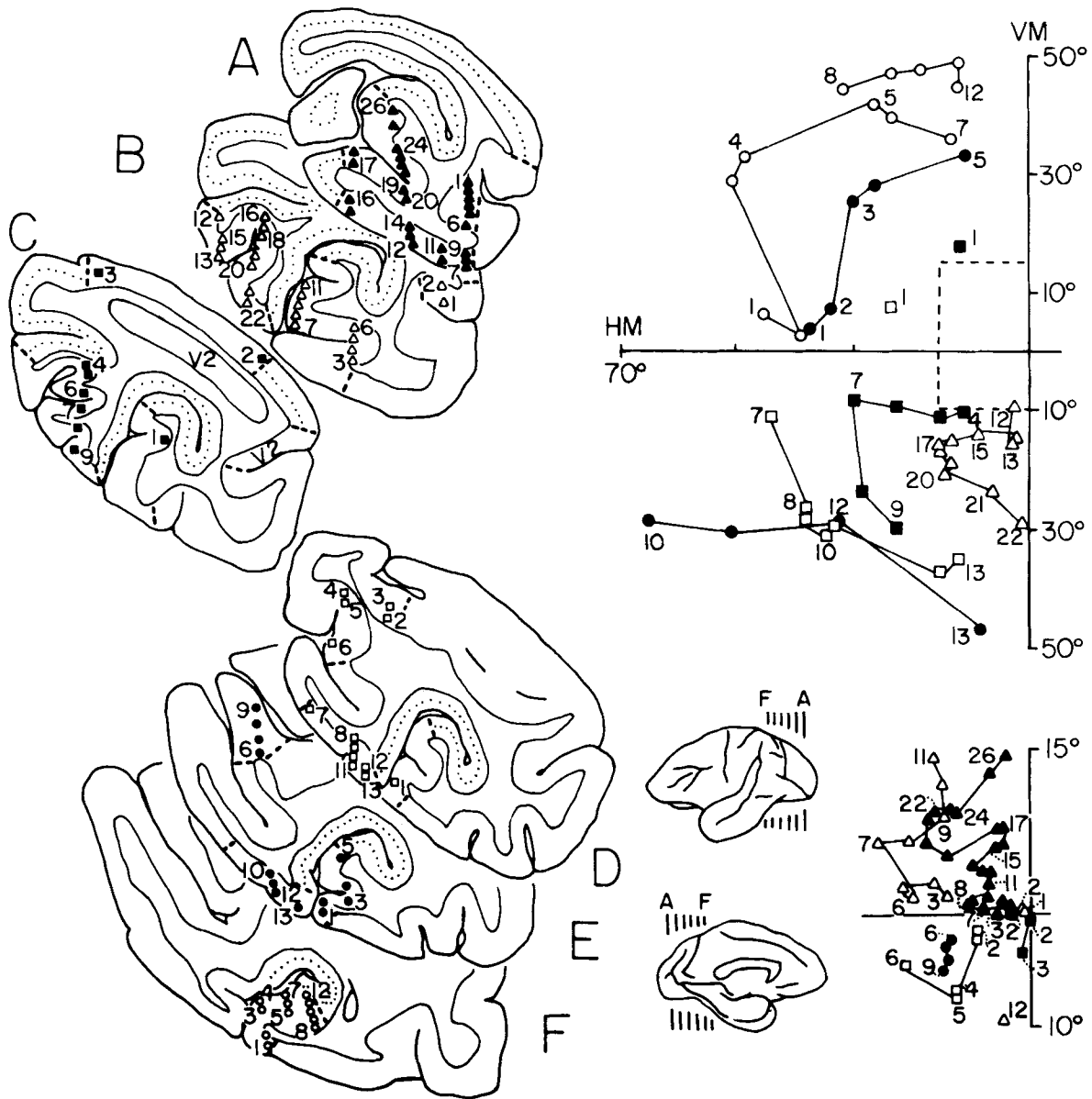


Fig. 3. Location of receptive field centers (right) corresponding to recording sites indicated on coronal sections (A-F) cut at the levels indicated on the lateral (upper inset) and medial (lower inset) views of the brain. The

region of representation of the central visual field (inside the dashed box) is magnified in the lower right (see also legend to Fig. 2).

with the same symbols used in Figure 2. In Figure 4C the eccentricities of the receptive field centers were placed at the location of the corresponding recording sites. The isoeccentricity lines were then drawn by eye to fit the values indicated in the map. In another map, using the values of the polar angle of the receptive field centers, we drew the location of the meridians and of the lines of + and -45° polar angle. These were combined in a more descriptive map of the visual topography in V2 for this animal in Figure 4D. In this figure, the extent of foveal V2 and the location of the split of HM were estimated on the basis of anatomical experiments from other animals (see below).

Although the sulcal pattern varies from animal to animal, the visual topography of V2 remains fairly constant across animals. Figure 5 compares the visual topography of V2 on flattened maps of two animals with very different

sulcal patterns. In spite of these variations in the sulcal pattern, the location, dimensions, and visuotopic organization of V2 are similar in both animals.

The extent of the visual field represented in V2 is shown in Figure 6. The hatched region represents the portion of the visual field delimited by the most nasal and most peripheral borders of the receptive fields recorded in V2 in seven animals. The dashed line corresponds to the mean extent of the monocular field of vision of three monkeys under neuromuscular paralysis, and the dotted line delimits the binocular field of vision. For the determination of the extent of the field of vision we followed the same procedure described by Gattass et al. ('87). As illustrated in Figure 6, V2 contains a representation of the entire binocular segment and at least part of the monocular crescent of the visual field. No receptive field centers were observed in

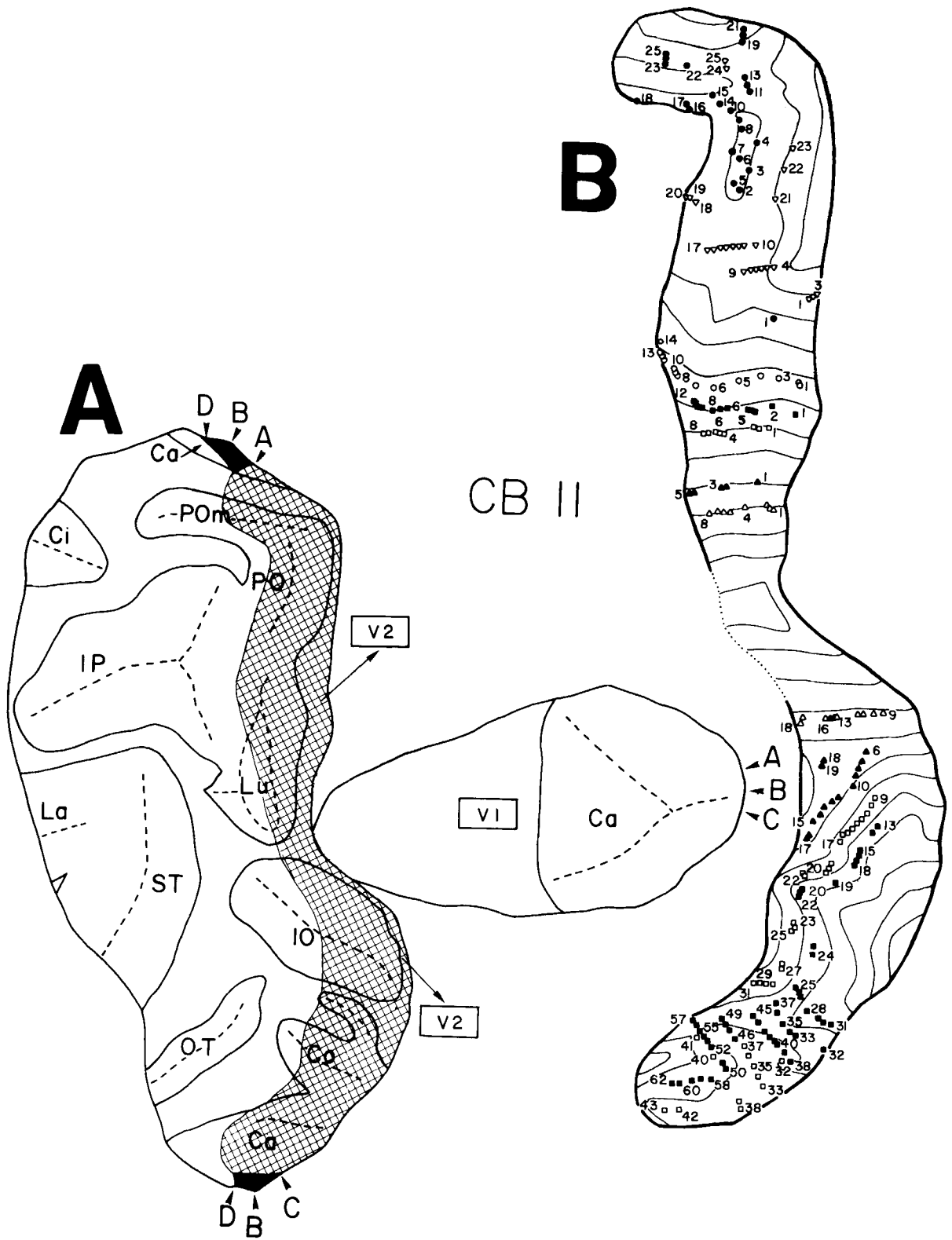


Fig. 4. A: Flattened reconstruction of striate and prestriate cortices, from the same animal illustrated in Figure 2, showing the location of V2 (hatch) and of area prostriata (black). B-D: Enlarged views of the flattened model of V2. For details see text.

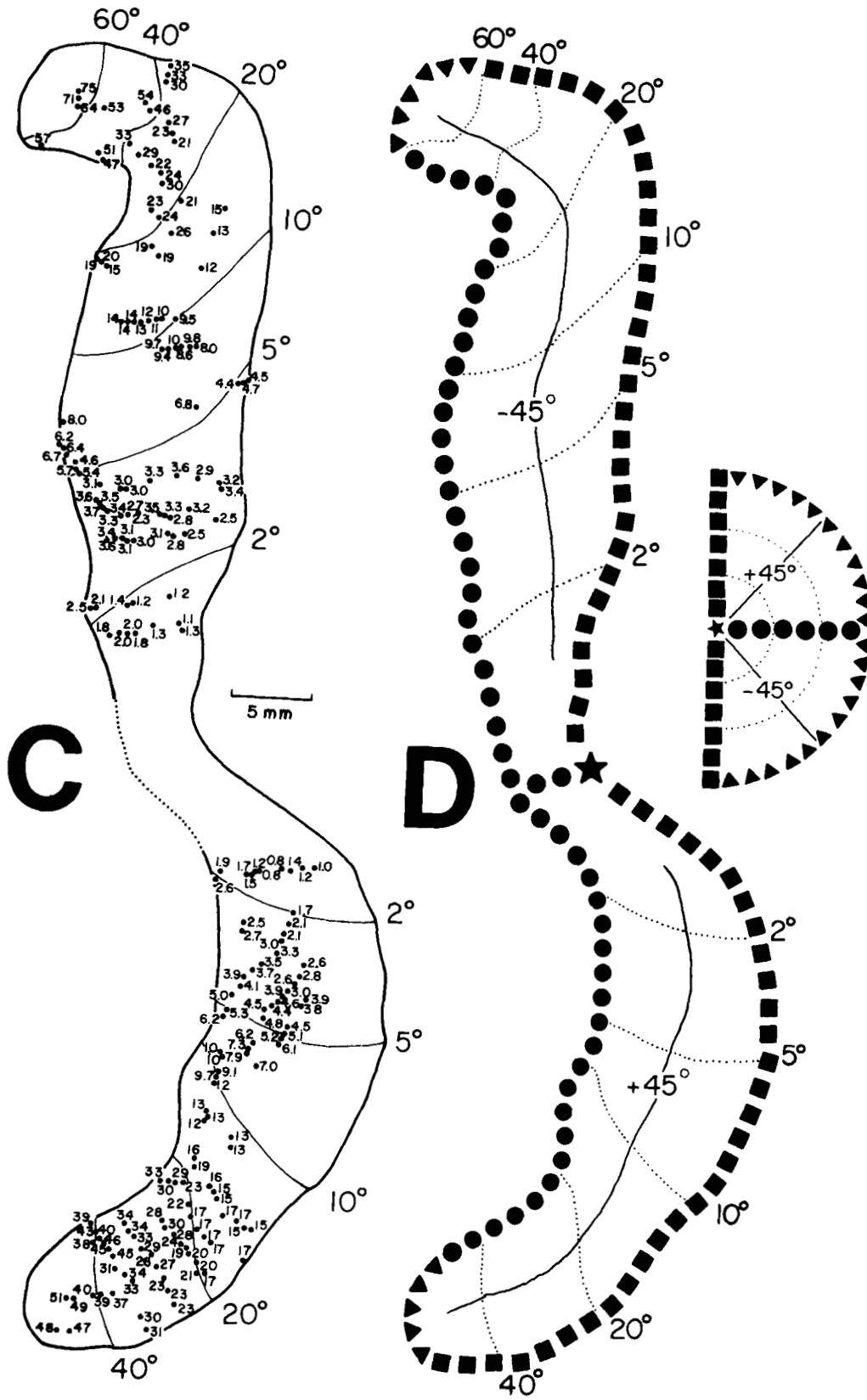


Figure 4 continued

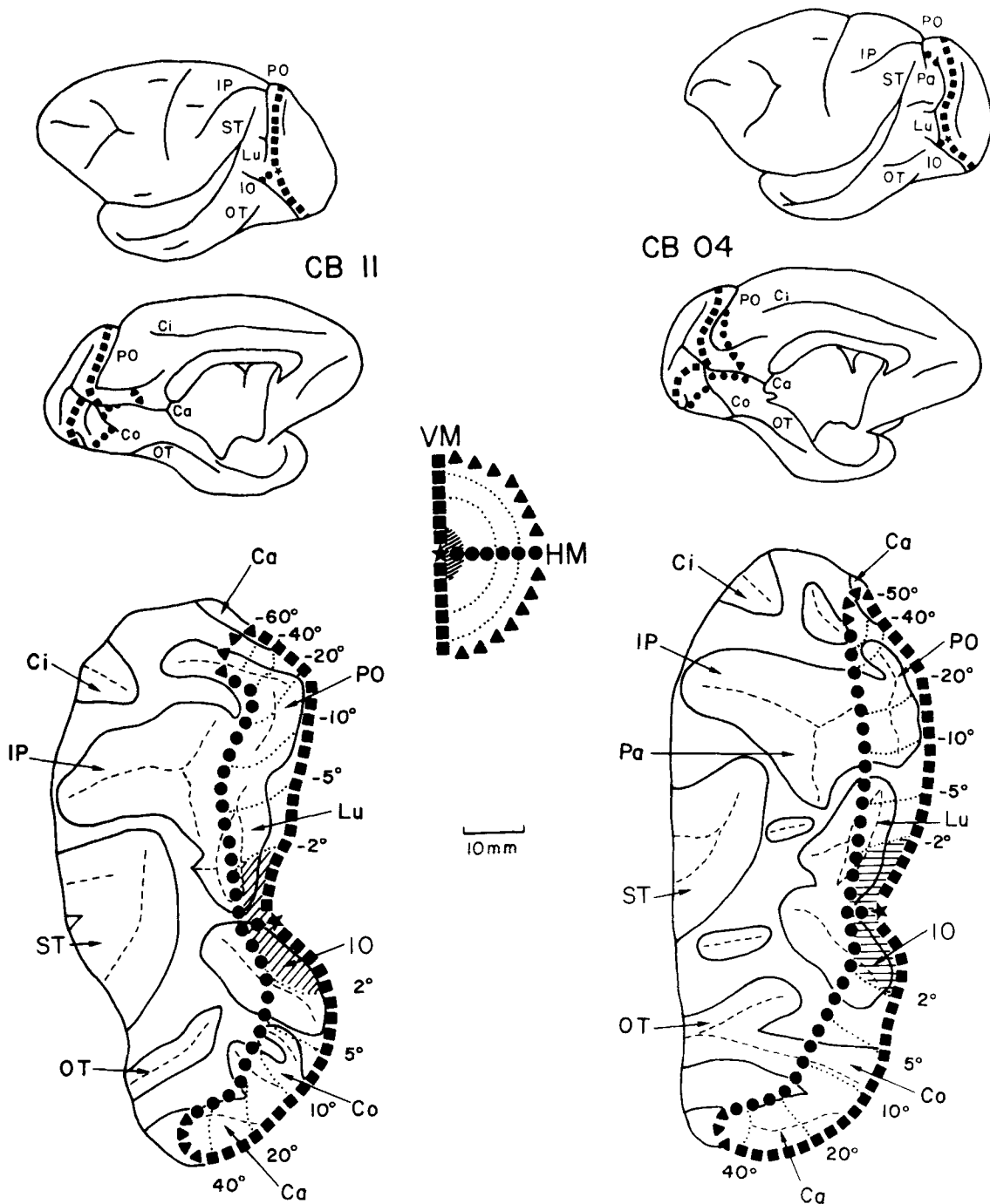


Fig. 5. Flattened maps of V2 in two animals with distinct sulcal patterns. Upper drawings are based on photographs of the dorsolateral and medial views of the brains of animals CB11 and CB04, where the positions of the

the ipsilateral hemifield, although the borders of some receptive fields occasionally invaded the ipsilateral hemifield by a few degrees.

Electrophysiological determination of the borders of V2

Abrupt changes in the progression of receptive field centers, as well as in receptive field sizes, were the criteria used to define the electrophysiological borders of V2.

meridians and of the center of gaze were drawn by eye. Lower drawings are flattened reconstructions of prestriate cortex showing the visuotopic organization of V2 relative to the sulcal pattern (see also legend to Fig. 1).

Figure 7 illustrates receptive fields recorded through dorsal and ventral V2 at the level of representation of the central visual field in a parasagittal section. As one moves along V2, from the border of V1 to the anterior border of V2 both dorsally (sites 5–11) and ventrally (sites 19–26), the receptive field positions change from the vertical to the horizontal meridian. After crossing the border between V2 and the anteriorly located visual area there is not only a reversal in field sequence but also an increase in field size.

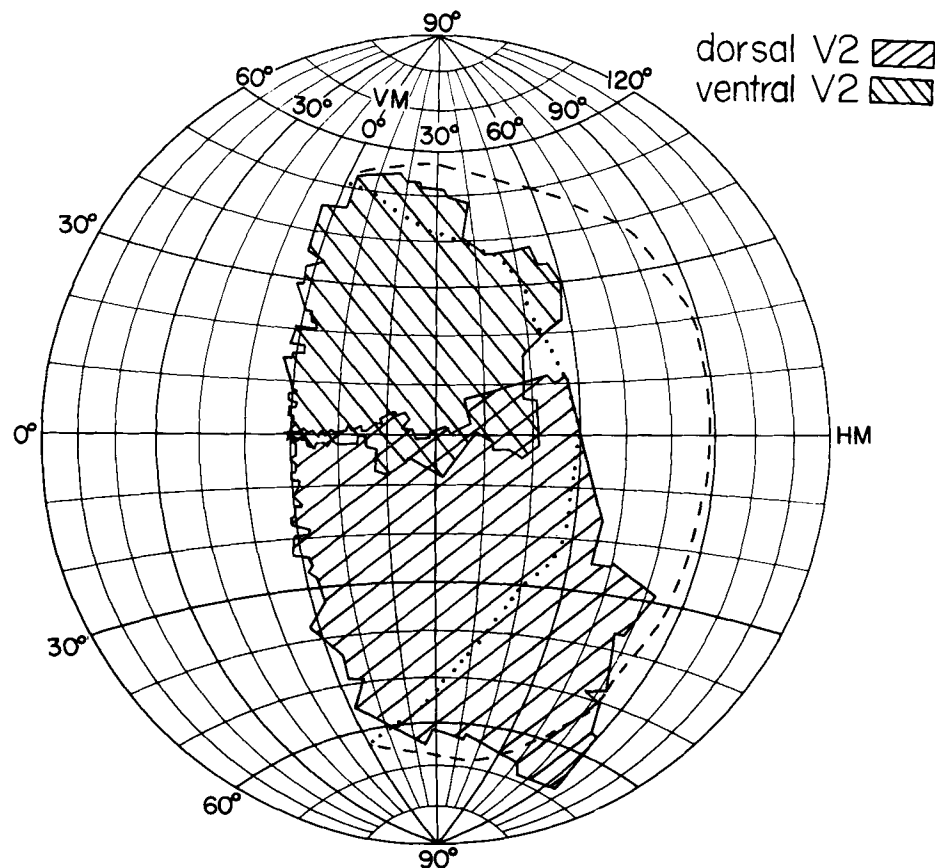


Fig. 6. Extent of the visual field represented in V2 (hatched). For details see text.

Figure 8 illustrates the borders of V2 with surrounding areas at the region of representation of the far periphery. Figure 8 upper left shows recording sites in an enlarged view of the calcarine sulcus at the level indicated in the medial view of the brain. Figure 8 lower left is a flattened reconstruction of the most anterior portion of the calcarine sulcus and adjoining ventral cortex. As shown in Figure 8 right, the border between V1 and V2 at more posterior levels represents the vertical meridian (sites 10 and 11). As one moves anteriorly along the lower bank of the calcarine sulcus the fields progress toward the periphery, and the V1/V2 border at this region no longer represents the vertical meridian. Instead, this border represents the far periphery (sites 8 and 15). As one moves toward the border between V2 and the ventrally located visual area, the receptive fields move toward the horizontal meridian (sites 11–22). After crossing the myeloarchitectonic border between V2 and the adjoining ventral area, the receptive fields begin to move away from the horizontal meridian. In this case, however, the increase in receptive field size is not as apparent as the one illustrated in Figure 7. Thus, the definition of the borders of V2 should rely on a combination of criteria.

Myeloarchitecture

In sections stained for myelin with the Heidenhain-Wöelcke method, V2, as defined electrophysiologically, is

myeloarchitectonically heterogeneous (Fig. 9). It shows myeloarchitectonic patterns which vary from less to more stratified. The less-stratified pattern is characterized by a thick and homogeneous band of fibers extending from layer VI to the bottom of layer III (Fig. 9A) and thus resembles the pattern previously described for V2 in the macaque (Gattass et al., '81). The more stratified V2 is characterized by a less-intense myelination of layer V so that the inner and outer bands of Baillarger become conspicuous (Fig. 9B). Another characteristic of the more stratified V2 is that the inner band is thicker than the outer band and it extends to the border with the white matter (Fig. 9B). Figure 10 shows the distribution of the patterns of myelination in V2 in two animals. The distribution of these patterns varies considerably from animal to animal. In all animals, most of V2 shows the less stratified pattern, and this is the only pattern observable in the region of representation of the periphery. The more stratified pattern predominates in central V2. The transitions between these patterns are usually gradual. In some animals this pattern of myelination resembles the distribution of the cytochrome oxidase bands demonstrated in tangential sections by Tootell et al. ('83). However, the regions presenting a stratified pattern of myelination are wider and less regularly distributed than the cytochrome oxidase bands demonstrated by these authors.

As described previously, V2 can be easily distinguished from V1 and area prostriata on the basis of both cyto- and

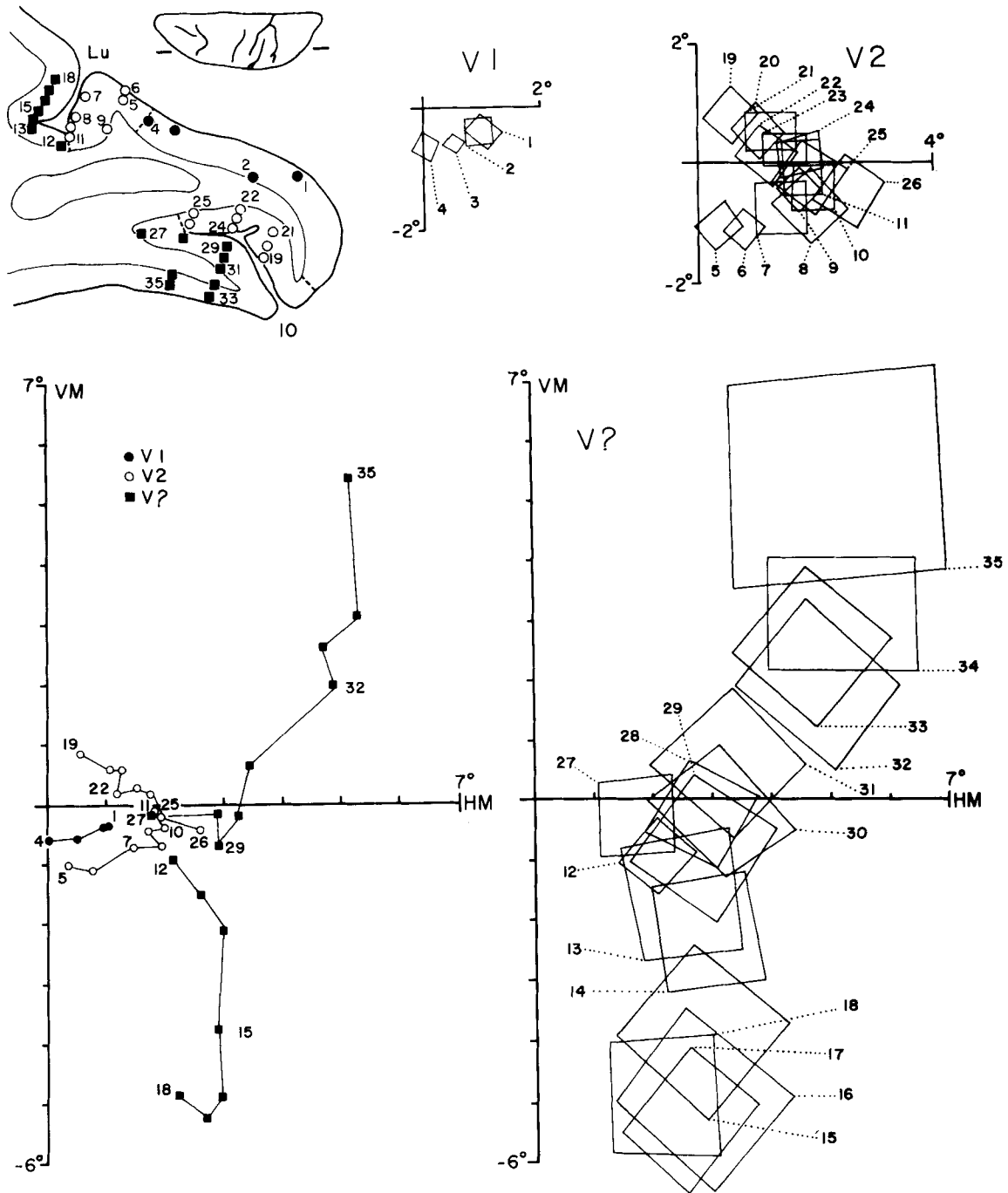


Fig. 7. Central receptive fields in V2 and neighboring areas. The recording sites are indicated on the parasagittal section cut at the level indicated on the dorsal view of the brain. The location of the centers of the receptive

fields recorded at these sites are shown in the lower left and the receptive fields in the upper right (V1 and V2) and lower right (V?). The dashed lines on the sections indicate the myeloarchitectonic borders of V2.

myeloarchitecture (Allman and Kaas, '71, '74; Sanides, '72; Gattass et al., '87). Most of the border of V2 with other areas of the prestriate cortex can also be determined in Heidenhein-Wöelcke stained sections. The determination of these borders is based on the characteristics of the inner and outer bands of Baillarger. Throughout V2 the outer band of Baillarger is not sharply defined. This characteris-

tic can be used to distinguish V2 from the cortex located ventral and laterally, which is clearly stratified and presents a thin, sharply defined outer band of Baillarger (Fig. 9C). In addition, these areas present a paler band between the inner band and the white matter, which is not observable in V2. V2 may also be distinguished from a medially located area which in addition to being densely myelinated,

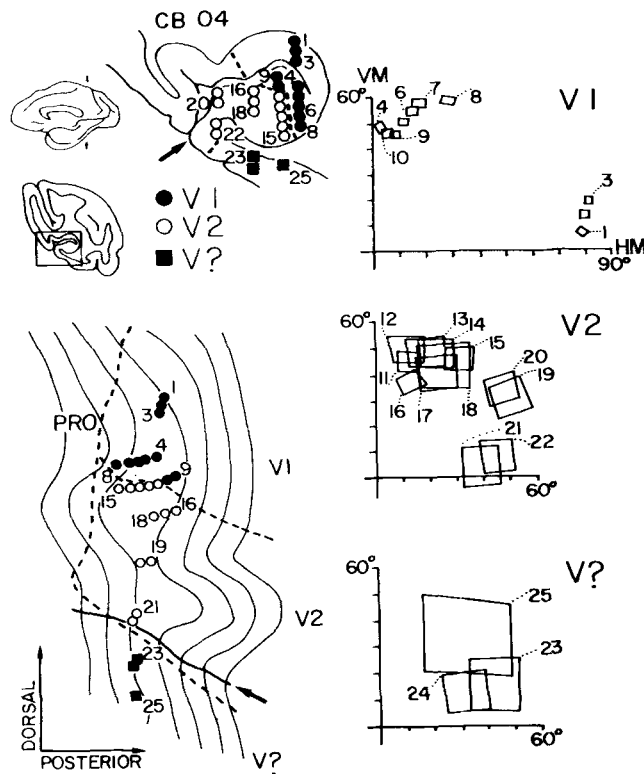


Fig. 8. Peripheral receptive fields in V2 and neighboring areas. The recording sites are indicated in an enlarged view of the calcarine sulcus cut coronally at the level indicated on the medial view of the brain (upper left) and on the flattened reconstruction of the anterior portion of the calcarine sulcus (lower left). The locations of the receptive fields are shown on the right. The dashed lines are myeloarchitectonic borders. Arrows indicate the lower lip of the calcarine sulcus. Lower left: Thin lines represent the contours of layer IV of the sections used to build the flattened reconstruction, and the heavy line indicates the lower lip of the calcarine sulcus.

presents a sharp, heavily myelinated, thick outer band of Baillarger (Fig. 9D). This area is visually driven (Neuenschwander et al., in preparation) and may correspond to area PO of the macaque (Covey et al., '82; Gattass et al., '86; Colby et al., '88).

In some animals, we were unable to distinguish the border of V2 at the posterior bank of the paraoccipital sulcus and anectant gyrus—regions which present a myelination pattern similar to that of peripheral V2. Likewise, the border of foveal V2 with anteriorly located prestriate areas is not always conspicuous. In this region, the areas usually present a pattern of myelination similar to that of the more stratified V2.

Split of the horizontal meridian and width of foveal V2

The borders of V2 are not equally well determined at all eccentricities. Several factors, such as the high magnification factor, receptive field scatter, and contiguity with the foveal representation of other areas converge to make the determination particularly difficult at the foveal representation. In addition, the determination of the anterior border of V2 at this region is not always clear based on myeloarchitectonic differences. For these reasons we have used anatomical tracers to help establish this boundary. Inasmuch as the connections between V1 and V2 in the macaque were shown to be homotopic (Weller and Kaas, '83),

one would expect that injection of a tracer along the horizontal meridian representation of V1, at an eccentricity below the value of horizontal meridian split in V2, would result in a single patch of label in V2. On the other hand, injections placed at higher eccentricities along the horizontal meridian in V1 would result in two distinct patches of label, one dorsal and one ventral, at the region of the horizontal meridian representation in V2. Therefore, two retrogradely transported fluorescent tracers were injected at different eccentricities along the representation of the horizontal meridian in V1. The data were charted on flattened reconstructions of the striate opercular surface and surrounding cortex to provide an overall view of the injection sites and projection zones as well as to allow direct measurements of the width of V2.

The upper part of Figure 11 illustrates the results obtained in animal CB09, in which the bisbenzimid injection at 0.5° eccentricity resulted in only one patch of labelled cells in V2 while the Nuclear Yellow one at 2.1° eccentricity resulted in two distinct patches: one in dorsal and the other in ventral V2.

The lower part of Figure 11 illustrates the results from two additional animals. In animal CB08 the injection at 2.5° resulted in two patches, while the injection at 0.8° resulted in a continuous patch. This patch, however, had two distinct, heavily labelled dorsal and ventral subregions. In case CB07, both injections (at 1.1 and 3.0° eccentricities) resulted in separate patches at the anterior region of central V2. These results indicate that the representation of the horizontal meridian splits at an eccentricity below 1° to form the anterior border of V2.

The projection from V2 to V1 is characterized by heavily labelled, densely packed cells at both infra- and supragranular layers. The cells labelled at areas anterior to V2, both dorsal and ventrally, are larger than those observed in V2, more sparsely distributed, and located mainly in the infragranular layers; rarely a few cells are also found in the supragranular layers (Piñon et al., '86). The region of transition in the laminar distribution of labelled cells was considered to be the border between V2 and the anteriorly placed area in the region of foveal representation. The coincidence between this anatomical transition and the anterior border of V2 was confirmed, at more peripheral eccentricities, by combined experiments involving tracer injections in V1 and electrophysiological recordings (Sousa et al., in preparation).

In the region of foveal representation, the width of V2 was measured on the flattened models from the cyto- and myeloarchitectonic border between V1 and V2, posteriorly, to the region of transition in the laminar distribution of labelled cells, anteriorly. The width of foveal V2 was smaller than at other eccentricities and varied from 4 to 5 mm.

Receptive field size

The variation of the square root of receptive field area as a function of eccentricity of receptive field center in V2 is shown in Figure 12. The linear function fitted to the data by the method of least squares, expressed by equation (1), provides a good description of the data.

$$\text{RF size} = 0.57 + 0.22 (\text{ecc}) \quad (R^2 = 0.73; n = 478) \quad (1)$$

Cortical magnification factor and anisotropy

The cortical magnification factor (CMF) in V2, i.e., the distance, in millimeters, between two recording sites di-

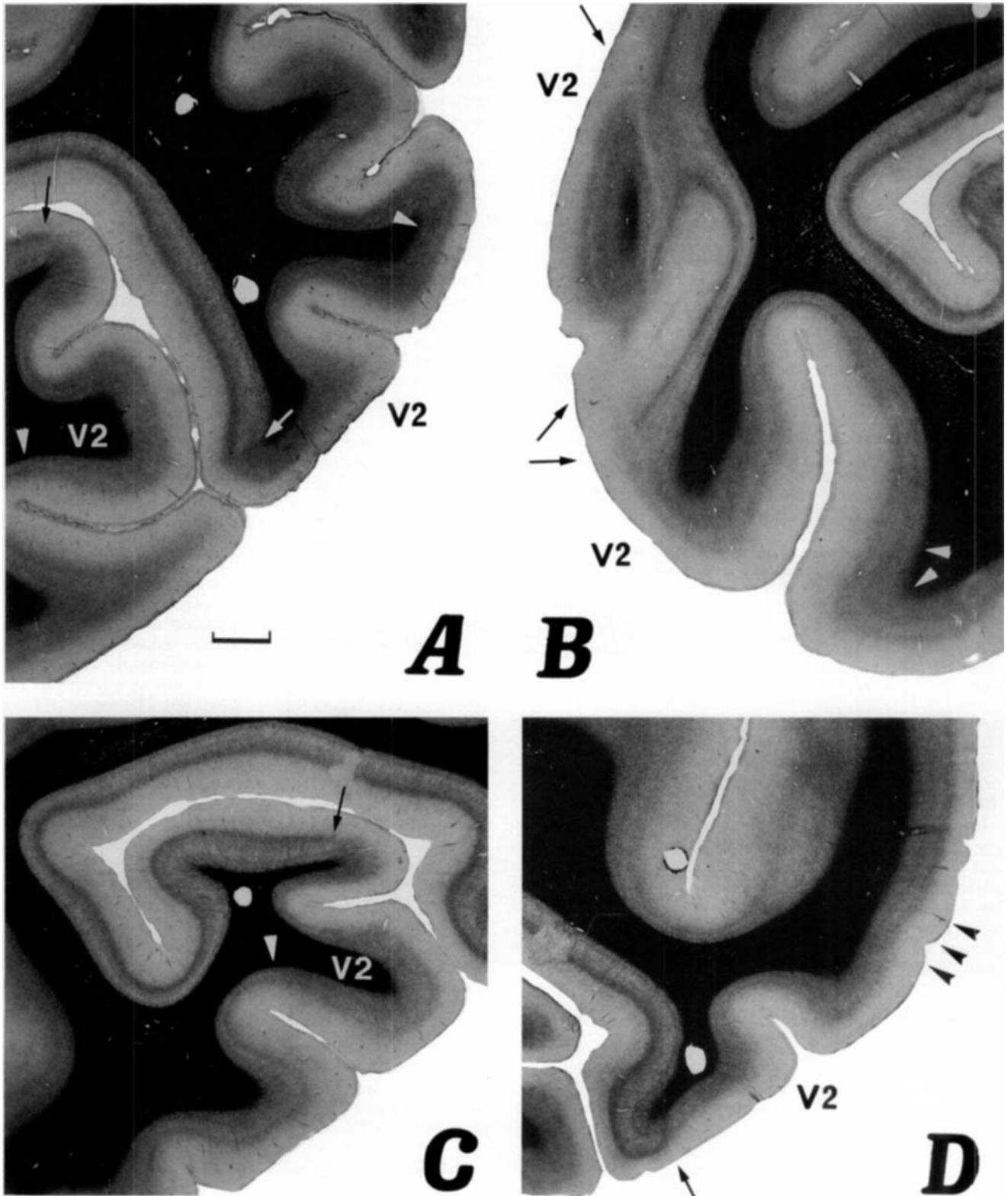


Fig. 9. Photomicrographs of myelin-stained coronal sections. Upper: The myeloarchitectonic patterns observed in peripheral (A) and central (B) V2. Lower: The borders of V2 with a ventrolateral (C) and a medial (D) visual area. Arrows point to the borders between V1 and V2; arrowheads indicate the borders between V2 and other visual areas. Gradual transitions are indicated by multiple arrowheads (for details see text). Scale bar = 1 mm.

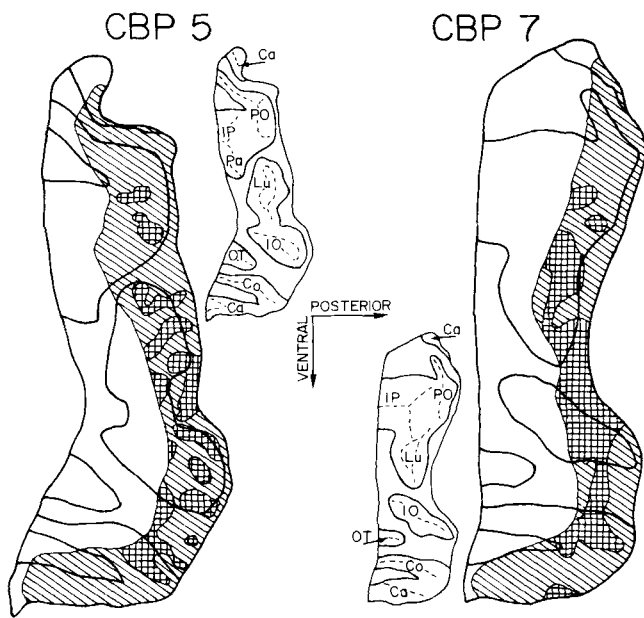


Fig. 10. Distribution of the patterns of myelination of V2 in two animals. Drawings are flattened reconstructions of prestriate cortex with V2 indicated in hatch. Simple hatch, less stratified pattern; crosshatch, more stratified and intermediate patterns. Insets are flattened reconstructions with sulci indicated. The dashed lines indicate the fundi of the sulci and the heavier lines the lips of the sulci.

vided by the distance, in degrees, between the centers of corresponding receptive fields (Daniel and Whitteridge, '61), was determined along different dimensions for two animals.

The cortical distance between two recording sites was directly measured on three-dimensional reconstructions of V2, following the same procedure used by Gattass et al. ('87). Inasmuch as in V2 two adjacent receptive fields immediately above and below the horizontal meridian can be separated by several millimeters along the cortical surface, the data for dorsal and ventral V2 were treated separately for the calculations of the CMF. The terms "isopolar CMF" and "isoeccentric CMF" refer to the CMF calculated with recording sites located along lines approximately parallel to the isopolar or isoeccentric lines in V2.

Power functions fitted to the isopolar CMF data for the upper and the lower quadrants were not statistically different (slope $t = 0.66$, $.5 < P < .55$; intercept $t = 0.38$, $.65 < P < .7$). Likewise, there was no difference between the functions fitted to the isoeccentric CMF data of either quadrant (slope $t = 0.29$, $.75 < P < .8$; intercept $t = 0.93$, $.3 < P < .35$). Thus, we have pooled the data of the two quadrants in the analysis of CMF in V2.

In both monkeys, power functions fitted to the CMF data measured along the isopolar (Mp) and isoeccentric (Me) dimensions in V2 had similar slopes (CB 04 $t = 0.08$, $.9 < P < .95$; CB 11 $t = 0.89$, $.35 < P < .4$), but different y intercepts (CB 04 $t = 12.51$, $P < .0001$; CB 11 $t = 14.98$, $P < .0001$) (Fig. 13). These results demonstrate the existence of an anisotropy in the representation of the visual field in V2, with Mp being about 1.5 times greater than Me at all eccentricities. Inasmuch as there was no significant difference between the CMF functions of each animal, we have pooled the data. Equations (2) and (3), represented in dashed line in Figure 13 A and B, respectively, describe the power functions of the variation of CMF with eccentricity in V2, fitted by the method of least squares.

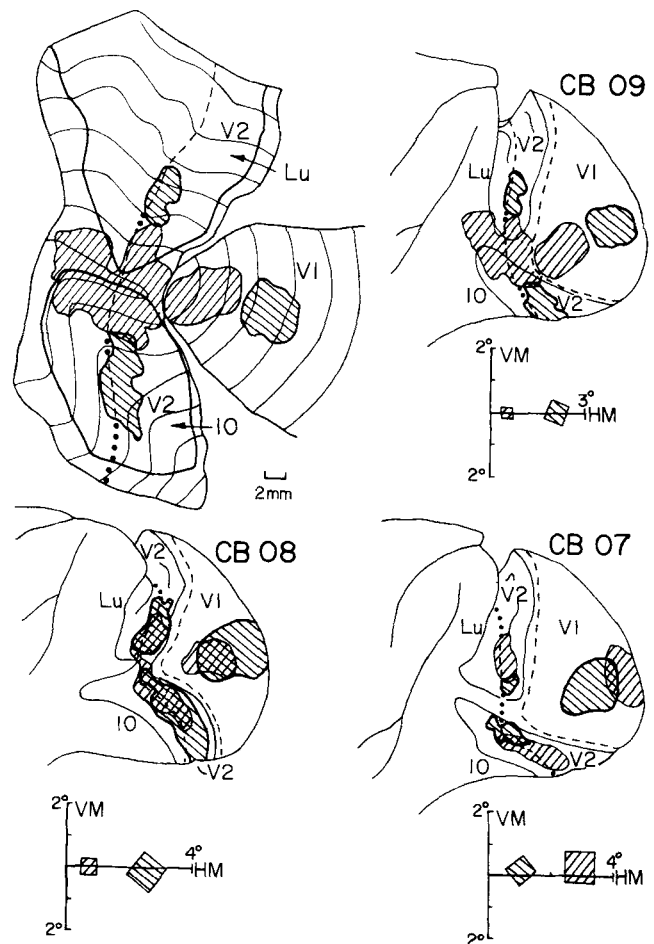


Fig. 11. Split of horizontal meridian representation in V2. Upper left, flattened reconstruction of the opercular region of V1 and of adjacent prestriate areas of animal CB09. Thin lines represent the contours of layer IV of the sections used to build the model. Thick lines indicate the lips of the sulci. Upper right and lower, schematic representations of the posterior portion of the brain of three animals with sulci partially opened. Injection sites and corresponding projection zones are hatched. Dashed lines indicate the borders based on the myeloarchitectonic pattern or on the laminar distribution of labelled cells. Dots are estimated borders. Insets show the receptive fields recorded at corresponding injection sites.

$$M_p = 10.31 (\text{ecc})^{-1.04} (R^2 = 0.92; n = 655) \quad (2)$$

$$M_e = 7.23 (\text{ecc})^{-1.06} (R^2 = 0.87; n = 649) \quad (3)$$

The power functions thus obtained tend to overestimate the values of the CMF at the regions of foveal and far peripheral representations. As in striate cortex (Gattass et al., '87), second-order polynomial functions fitted to the natural logarithms of both magnification factor and eccentricity were found to be more adequate to describe the CMF data. These functions (equations [4] and [5]) are represented as continuous lines in Figure 13A and B, respectively.

$$\text{Ln}(M_p) = 1.97 - 0.63 (\text{Ln}[\text{ecc}]) - 0.09 (\text{Ln}[\text{ecc}])^2 \quad (4)$$

$$(R^2 = 0.93)$$

$$\text{Ln}(M_e) = 1.69 - 0.75 (\text{Ln}[\text{ecc}]) - 0.07 (\text{Ln}[\text{ecc}])^2 \quad (5)$$

$$(R^2 = 0.88)$$

The areal cortical magnification factor (ACMF), i.e., the ratio of the area of a given region of the cortical surface in square millimeters, and the area of the corresponding segment of the visual field in square degrees (Tusa et al., '79)

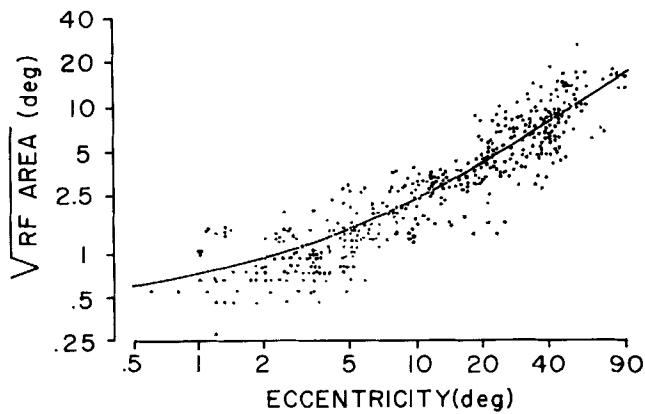


Fig. 12. Receptive field size as a function of eccentricity of receptive field center in seven animals (for details see text).

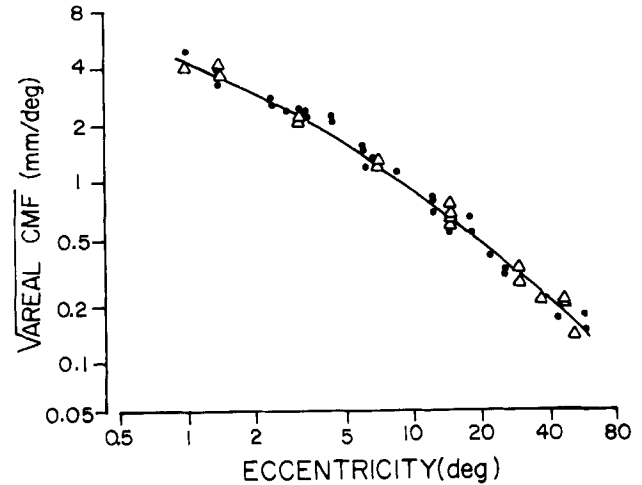


Fig. 14. Square root of the areal cortical magnification factor as a function of eccentricity for the same animals illustrated in Figure 13 (for details see text).

$$\begin{aligned} \text{Ln}(\sqrt{\text{ACMF}}) &= 1.55 - 0.51(\text{Ln}[\text{ecc}]) \\ &\quad - 0.10(\text{Ln}[\text{ecc}])^2 \end{aligned} \quad (6)$$

$(R^2 = 0.99; n = 74)$

DISCUSSION

Visuotopic organization

The visual topography of V2 in the *Cebus* is similar to that described for the nocturnal platyrrhine *Aotus* (Allman and Kaas, '74) and for the diurnal catarrhine *Macaca* (Gattass et al., '81). The visual field representation is not continuous: the upper visual quadrant is primarily represented in ventral V2 and the lower quadrant in dorsal V2. In fact, since our results demonstrate that at the anterior border of both dorsal and ventral V2 the visual representation may invade the opposite quadrant, in *Cebus* there is a redundant representation of the vicinities of the horizontal meridian (Fig. 6). This observation adds a new feature to the model proposed by Allman and Kaas ('74) for V2 in the owl monkey. The existence of receptive fields with centers in the upper quadrant, corresponding to sites located in the border of dorsal V2 with V3 in the macaque, was described by Zeki and Sandeman ('76) and Van Essen and Zeki ('78). In addition, Gattass et al. ('81) have also observed an invasion of the lower quadrant at the anterior border of ventral V2 in the macaque. These previous observations lend generality to our results.

These invasions are not due to eye movements, since we have monitored the position of the fovea throughout the experimental sessions. Furthermore, residual eye movements in macaques paralyzed with pancuronium bromide reach at most 0.5 degrees (Blasdel and Fitzpatrick, '84); thus, invasions of receptive field centers beyond the horizontal meridian extending up to 5° are unlikely to be explained by these movements.

What could be the functional role of the redundant representation of the horizontal meridian at the anterior border of V2? One hypothesis is that neurons in this region might be involved in signalling the coherence of the visual image across the horizontal meridian, subserving a similar function to that of callosal fibers for neurons with receptive fields close to the VM. This hypothesis is supported by the demonstration of modulatory peripheries in single-unit receptive fields of areas V2, V4, and middle temporal (MT) in the macaque (Moran et al., '83; Allman et al., '84; De Yoe

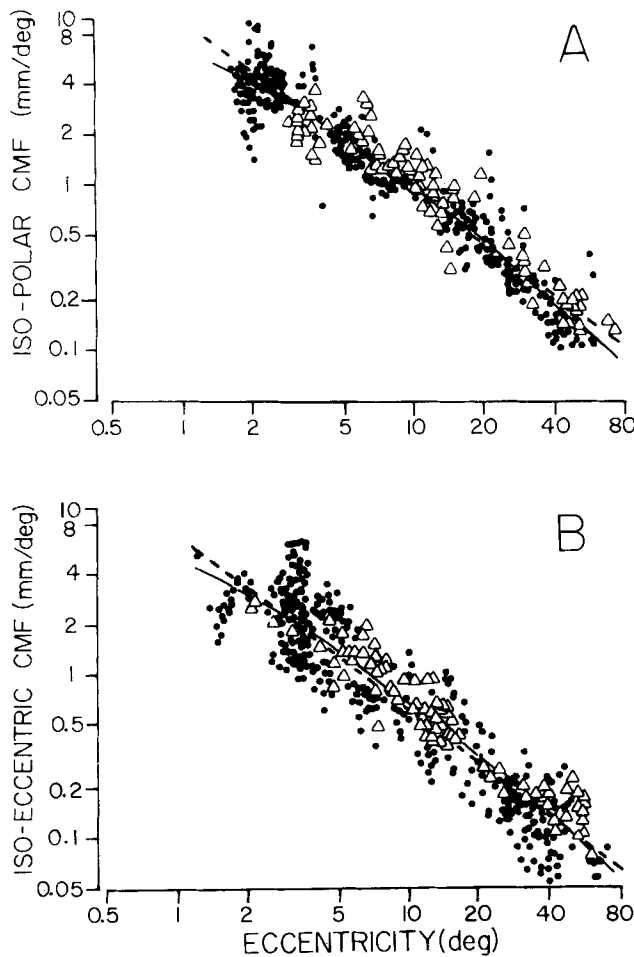


Fig. 13. Cortical magnification factor along the isopolar (A) and isoeccentric (B) dimensions as a function of eccentricity. Data from two animals: triangles, CB04; dots, CB11 (for details see text).

was determined with a method similar to that described by Gattass et al. ('87). Equation (6) corresponds to the best-fitting second-order polynomial function which describes the variation of $\sqrt{\text{ACMF}}$ with eccentricity in V2. The corresponding function is shown in Figure 14.

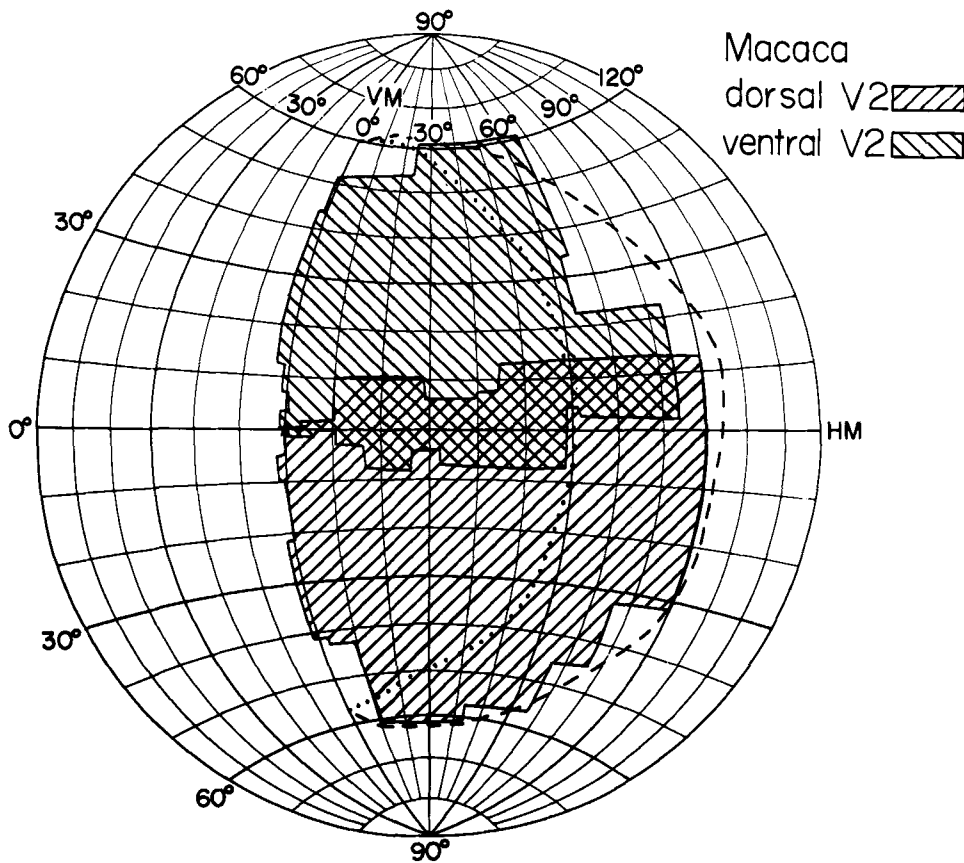


Fig. 15. Extent of the visual field represented in V2 in the macaque. Based on unpublished data from the work of Gattass et al. ('81; see also legend to Fig. 6).

et al., '86; Tanaka et al., '86). In V4, the interhemispheric connections provide the modulatory input which integrates the visual image across the vertical meridian (Moran et al., '83). In areas with second-order representations of the visual field there is a similar problem concerning the coherence of the visual image across the horizontal meridian. The double representation of a region in the vicinities of the horizontal meridian in V2 could provide the modulatory inputs to neurons with receptive fields near the horizontal meridian. Thus, there would be no need for long connections between dorsal and ventral portions of V2, although interconnections between dorsal and ventral area 18 in *Saimiri* have been described by Tigges et al. ('74).

In addition, as previously reported (Gattass et al., '81), we observed a small invasion of the ipsilateral hemifield in V2 which is consistent with the existence of a band of callosal connections in the border region between V1 and V2 (Van Essen et al., '82; Cusick et al., '86; Gould et al., '87). This invasion differs from that observed along the HM in that we have never observed receptive field centers in the ipsilateral hemifield.

Extent of the visual field represented in V2

The second visual area of the *Cebus* contains, in each hemisphere, a representation of the whole binocular segment and of at least part of the monocular crescent of the contralateral hemifield (Fig. 6). This result confirms previous electrophysiological reports by Allman and Kaas ('74) in the *Aotus* and by Gattass et al. ('81) in the macaque. On the other hand, based on cytochrome oxidase topography,

Tootell et al. ('85), who questioned the presence of a representation of the monocular crescent in V2, suggested that the region containing cytochrome oxidase strips is coextensive with the region of binocular representation in V2. The existence of a predominance of color- and disparity-sensitive neurons in cytochrome oxidase-rich strips (Hubel and Livingstone, '85) suggests an alternative explanation: it is conceivable that the pattern of strips does not extend to the periphery of V2, where one finds the representation of the monocular crescent.

In the present report we did not record receptive fields in the upper monocular crescent in V2. According to the model proposed by Allman and Kaas ('74) the region representing the upper monocular crescent should be located at the anterior portion of the lower bank of the calcarine sulcus. If one considers that the theoretical distance between the isoecentricity lines for 60 and 80°, based on the isopolar CMF, is 3.1 mm, one could assume that the unexplored region in this study, at the anterior portion of the lower bank of the calcarine sulcus, is only slightly smaller than that needed to accommodate the representation of the upper monocular crescent (see Fig. 4). Therefore, our results are compatible with the existence in V2 of a complete representation of the field of vision of the monkey in the paralyzed condition, as previously reported by Allman and Kaas ('74) and Gattass et al. ('81). Inasmuch as the existence of a representation of the monocular crescent in V2 has been recently questioned (Tootell et al., '85), we illustrate in Figure 15 the extent of the visual field represented in dorsal and ventral V2 in the macaque, based on unpub-

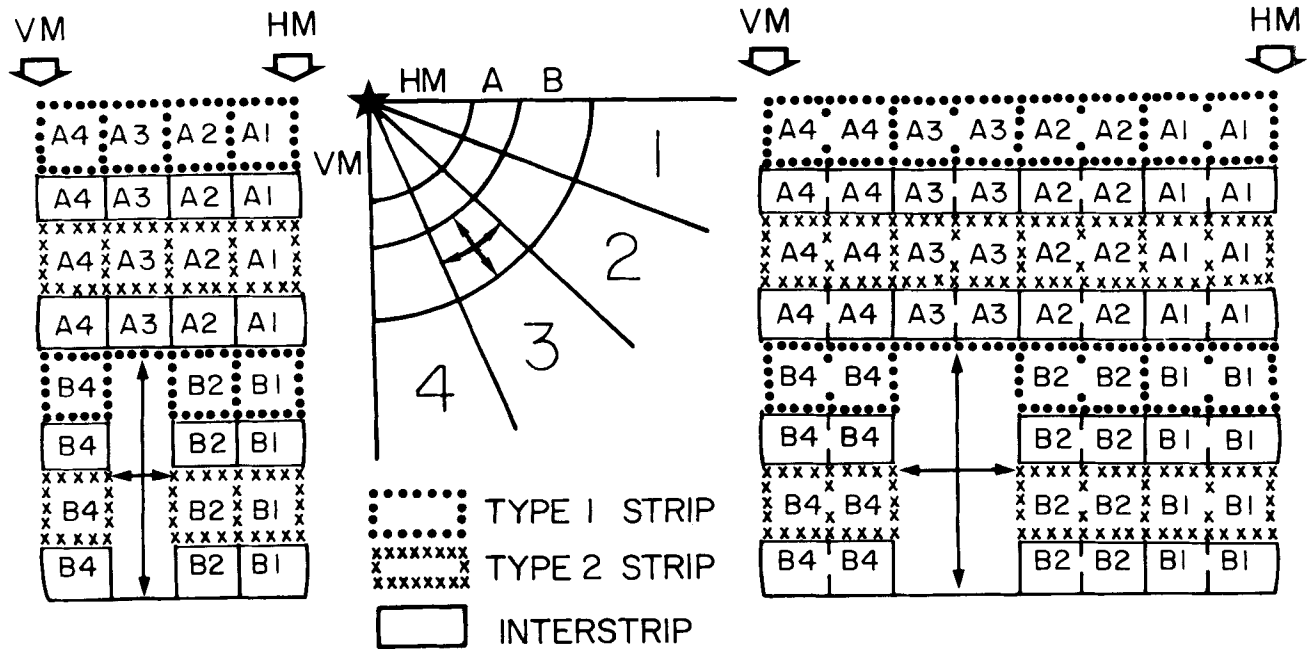


Fig. 16. Theoretical models of the local visuotopic organization in V2. **Middle:** Representation of a quadrant of the visual field with two isoeccentric (A, B) and four isopolar (1-4) sectors indicated. Arrows in sector B3 indicate equal displacements along the isoeccentric and isopolar dimensions

in the visual field. **Left and right** are models of the representation, in V2, of the visual sectors illustrated in the middle with respect to cytochrome oxidase band pattern. Open arrows point to the representation of the meridians (for details see text).

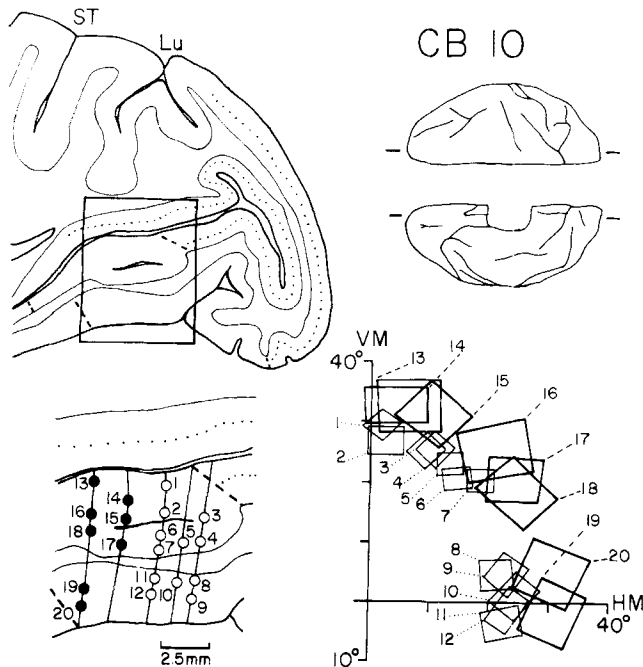


Fig. 17. Bands of isoeccentric representation in V2. **Upper left**, parasagittal section cut at the level indicated on the dorsal and ventral views of the brain (**upper right**). The region inside the box is magnified in the **lower left** with the recording sites indicated. **Lower right**, location of receptive fields recorded at the sites indicated in the lower left.

lished data from the study of the visuotopic organization of V2 by Gattass et al. ('81).

Size of V2

Studies of V2 in macaque and owl monkeys yielded conflicting results concerning the relationship between the sizes of V1 and V2. Based on data reported by Gattass et

al. ('81) and Van Essen et al. ('86) in the macaque, the area of V2 was found to correspond to approximately 80% of that of V1. For the owl monkey, the area of V2 reported by Tootell et al. ('85) is compatible with that obtained based on electrophysiological data (Allman and Kaas, '74). According to these data the ratio between the areas of V2 and V1, in *Aotus*, is much smaller (about 25%). In the *Cebus*, the ratio between the areas of V2 and V1 was found to be approximately the same as that reported for the macaque. In addition, the absolute size of V2 in the *Cebus* has been found to be similar to that reported for the macaque (Gattass et al., '81; Van Essen et al., '86).

The difference in the ratio of the areas of V2 and V1 in *Cebus* and *Macaca* in comparison with that observed in *Aotus* is puzzling in view of the fact that the ratio between the areas of MT and V1 is nearly the same for the three above-mentioned species (Fiorani, '86). This observation suggests that the organization of the cortical visual areas of the *Aotus* does not result from a homogeneous compression of that observed in large, diurnal monkeys.

Boundaries of foveal V2 and split representation of the horizontal meridian

We were unable to precisely locate the anterior border of foveal V2 based both on electrophysiological and myeloarchitectonic criteria. Therefore, we have used the pattern of laminar distribution of labelled cells in prestriate areas following injections of retrograde tracers in V1 (Sousa et al., '87). Based on this method we concluded that V2 is a continuous belt, not segregated in dorsal and ventral portions. This result was further confirmed by the presence of cytochrome-oxidase-rich strips in the region of foveal representation anterior to V1 (Rosa et al., '88)—a pattern similar to that described for V2 by Tootell et al. ('83, '85). The split of the horizontal meridian representation in V2 was first demonstrated by Allman and Kaas ('74) in the owl monkey by means of electrophysiological recordings. These authors have demonstrated that in *Aotus* the representa-

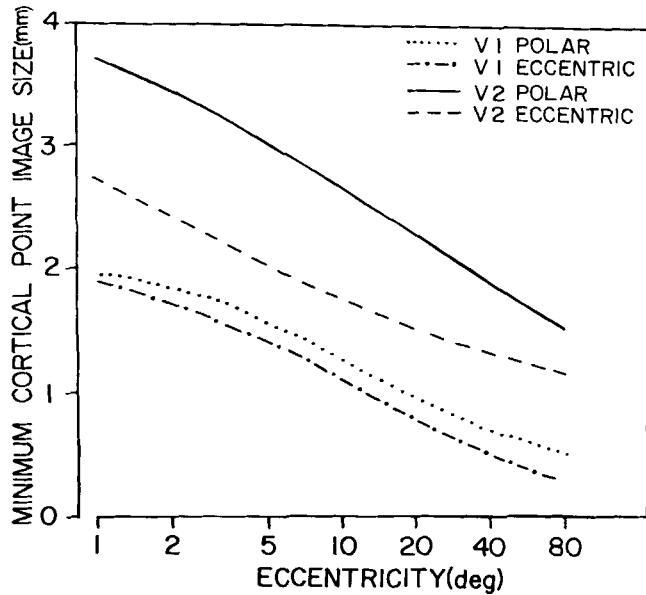


Fig. 18. Minimum cortical point image size as a function of eccentricity along the isopolar and isoecentric dimensions for V1 and V2. Data from two animals.

tion of the horizontal meridian is continuous with that of V1 up to an eccentricity of 7°, where it splits to form the anterior border of V2. In *Macaca*, the greater magnification factor of foveal V2 made it difficult to precisely determine the eccentricity at which the horizontal meridian representation splits. Based on the mean position of receptive fields in the region of foveal representation, Gattass et al. ('81) estimated that the split of the horizontal meridian occurs at approximately 1° eccentricity. In the present study, we have addressed this question by the use of retrograde tracers. Our results indicate that the representation of the horizontal meridian in V2 splits below 1° eccentricity and support the view of Gattass et al. ('81) that the more central split in macaques is related to greater foveal magnification factor in diurnal monkeys.

Cortical magnification factor and anisotropy

The variation of the areal cortical magnification factor with eccentricity for V2 has a smaller slope than that described for V1 (V1, -0.94 ; V2; -1 ; $t = 3.47$, $P < .0005$). While in the central visual field representation the mean cortical magnification factor is very similar for both V1 and V2, in the peripheral representation the values are greater for V1. Thus, the difference in the sizes of V1 and V2 could be the result of a compression in the peripheral representation of V2.

The magnification factor was not systematically studied at the foveal representation. Therefore, we cannot assign precise values of areal cortical magnification factor (ACMF) to specific eccentricities below 2°. However, equation (6) predicts a surface of 122.8 mm² for the representation of eccentricities between 4' and 120', a value that is compatible with that measured on partially unfolded models of V2 following the procedure described by Gattass et al. ('87). According to equation (6), the maximum $\sqrt{\text{ACMF}}$ value in V2 would be 9.3 mm/deg, at 4' eccentricity. This value is very similar to that estimated for V1 in the *Cebus* (9.6 mm/deg) at a similar eccentricity.

The comparison of the CMF functions in the isopolar and isoecentric dimensions revealed an anisotropy in the map

of the visual field of V2. For all eccentricities, the isopolar CMF is about 50% greater than the isoecentric one. This anisotropy could result from the existence, in V2, of three systems of cytochrome oxidase bands which are arranged in a pattern perpendicular to the border between V1 and V2, as described by Tootell et al. ('83). These strips are approximately parallel to the isoecentricity lines and perpendicular to the isopolar lines. Inasmuch as each type of strip is characterized by different single-unit properties and patterns of connections (Hubel and Livingstone, '85; De Yoe and Van Essen, '85; Shipp and Zeki, '85), it is conceivable that a given sector of the visual field may be represented many times in V2 at adjacent regions of different strips, as illustrated in Figure 16 for sector B3. Figure 16 illustrates theoretical models of the local visuotopic organization in V2 where segments of the visual field are rerepresented in each set of strips. In this model the position of the borders of each sector relative to the band pattern is an arbitrary one. The model illustrated in Figure 16 left implies an anisotropic representation of the visual field inasmuch as a given distance in the visual field would correspond to a cortical distance in the isopolar dimension on the average four times greater than in the isoecentric one. If one takes into consideration the heterogeneities within the cytochrome-oxidase-rich strips described by Wong-Riley and Carrol ('84) and by Shipp and Zeki ('85), one would arrive at a model similar to that illustrated in Figure 16 right. In this model, the heterogeneities along each strip would imply a remapping of each visual field sector so that each V2 "module," i.e., the cortical compartment capable of processing all information from a given point of the visual field, would be composed of eight subunits organized as illustrated. Without taking into account the differences in width of the strips this model predicts an anisotropy of approximately 2:1. Our data reveal an anisotropy of 1.5:1, a value which is only slightly smaller than that predicted by the second model proposed. This difference could be explained by the observation that the isoecentricity contours are not exactly parallel to the cytochrome oxidase bands found in the *Cebus* (unpublished observations).

Following this model, which is consistent with data presented in Figures 2a and 17, the topographic organization of V2 would not reflect a continuous, point-to-point transformation of the visual field. Instead, it would be a mosaic of discrete regions of representation of sectors of the visual field. Thus, one would expect a local disorderliness in the map of the visual field such that a displacement of several millimeters in the cortex would not always result in a predictable change in receptive field position. As illustrated in Figure 17, a displacement of recording sites in the anteroposterior dimension, along the lower bank of the calcarine sulcus, does not yield a smooth centroposterior displacement of receptive fields. Instead, receptive fields from the three posteriorly located penetrations (fields 1-12) tend to cluster in an almost isoecentric sector of the visual field, in spite of a 2.5-mm anteroposterior displacement along the cortical surface. Similarly, receptive fields from the two anteriorly located penetrations (fields 13-20) represent a more peripheral isoecentric sector of the visual field. In contrast with this discrete centroposterior displacement, a dorsoventral displacement of recording sites yields a smooth change in receptive field positions from the vertical to the horizontal meridian. Figure 2a also illustrates a discontinuous change in receptive field eccentricities as one crosses V2 in the centroposterior direction. The receptive fields corresponding to sites located in the poste-

In the retina of the adult albino rat, two classes (1 and 2) of TH-IR amacrine cells are recognized. The somata of class 1 TH-IR cells average approximately 13 μm in diameter (range, 10–22 μm), and are mostly found in the innermost part of the INL; a small minority are found in either the GCL, IPL, or in the outer part of the INL (Ehinger, '76, '83a,b; Nguyen-LeGros et al., '83, '84a, '86; Mitrofanis and Stone, '86; Versaux-Botteri et al., '86; Mitrofanis et al., '88b). Each class 1 cell has several thick beaded dendrites which mainly spread in several of the outer strata of the IPL. The dendrites of a minority of these cells spread in a middle stratum of the IPL (Nguyen-LeGros et al., '83, '84a, '86; Versaux-Botteri et al., '86). The dendrites of TH-IR cells spreading in the outer strata of the IPL frequently form "dendritic rings" around noncatecholaminergic somata at the border of the INL and IPL (Nguyen-LeGros et al., '83, '84a, '86; Mitrofanis and Stone, '86; Versaux-Botteri et al., '86; Mitrofanis et al., '88b). In the cat retina, these noncatecholaminergic somata are presumed to be those of the AII rod amacrine cells (Pourcho, '82). A small minority of class 1 TH-IR somata in the innermost part of the INL have a sclerally directed process terminating in the outer plexiform layer (OPL; Nguyen-LeGros et al., '81a,b; Versaux-Botteri et al., '86; Mitrofanis et al., '88b) and are considered to be interplexiform cells. Similar cells have also been described in other mammalian and nonmammalian retinas (Ehinger, '76, '83a,b; Dowling and Ehinger, '78; Frederick et al., '82; Nguyen-LeGros et al., '84b; Oyster et al., '85; Mitrofanis et al., '88b).

The class 2 TH-IR cells of the rat retina have small somata, averaging approximately 6 μm in diameter (range, 3–7 μm), located in the inner part of the INL. Their fine processes spread in a middle stratum of the IPL (Nguyen-LeGros et al., '83, '84a, '86; Mitrofanis and Stone, '86; Versaux-Botteri et al., '86; Mitrofanis et al., '88b).

The somata of ChAT-IR cells in the retina of the rat are numerous in both the GCL and INL, with a small majority in the GCL (Voigt, '86; Mitrofanis and Stone, '87a, '88). The dendrites of ChAT-IR somata in the GCL spread in an inner stratum of the IPL, whereas those in the INL spread in an outer stratum (Kondo et al., '85; Voigt, '86; Mitrofanis and Stone, '87a, '88). Masland et al. ('84) and Tauchi and Masland ('84) have argued that the inner population of ChAT-IR cells are important in the generation of ON-responses from ganglion cells, and the outer population in the generation of OFF-responses.

The distribution of ChAT-IR cells in the retina of the adult rat shares several features of the distribution of ganglion cells. The density of ChAT-IR cells is maximal in the region of peak ganglion cell density and declines toward the periphery (Voigt, '86; Mitrofanis and Stone, '87a, '88). Both classes of TH-IR cells, by contrast, concentrate in a broad area close to the superior temporal margin (Mitrofanis and Stone, '86; Mitrofanis et al., '88b). A similar distribution of TH-IR cells has been observed in the retinas of the cat, guinea pig, and hamster (Mitrofanis and Stone, '86; Mitrofanis and Finlay, '88; Mitrofanis et al., '88b).

In the present study, we have traced the postnatal development of TH- and ChAT-IR cells in the retina of the rat. Particular emphasis was placed on: (1) the age at which the cells first express their biosynthetic enzyme; (2) the development of the sublamination of their dendrites in the IPL, and (3) the development of their soma size, number, and distribution. In addition, their development was related to that of the ganglion cells with regard to soma growth and distribution.

A preliminary analysis of this work has been published in abstract form (Mitrofanis and Stone, '87b; Mitrofanis et al., '88a).

MATERIALS AND METHODS

Retinas were obtained from adult and postnatal albino (Wistar) rats aged at daily intervals between P0 (day of birth) and P24. Animals were given an overdose of Nembutal (60 mg/ml), and perfused transcardially with 10–200 ml of 0.1 M phosphate buffer (PB, pH 7.4) followed by a picric acid/formaldehyde fixative (Zamboni and De Martino, '67). The superior surface of each eyeball was marked with a felt pen and later by an incision for orientation. Eyeballs were enucleated and the cornea and lens removed. The eyecups were then immersed in a fresh solution of fixative for approximately 20 minutes. Retinas were dissected free in one piece, washed in phosphate-buffered saline (PBS; pH 7.4) containing 1% Triton X-100 (Ajax) and 10% fetal bovine serum for 1 hour, and subsequently incubated in: (1) rabbit serum containing anti-TH (Eugene Tech. Int., 1:2,400), or rat monoclonal anti-ChAT (Boehringer, Mannheim, 2–4 $\mu\text{g}/\text{ml}$), for 48 hours at 4°C; (2) biotinylated antirabbit or antirat Ig (Vectastain, Vector Labs., 1:50) for 2 hours at room temperature; (3) the avidin-biotin-peroxidase complex (Vectastain, Vector Labs.) for 1 hour at room temperature; and (4) a nickel-enhanced, 3,3'-diaminobenzidine (Sigma) solution (Adams, '81). Along with retinas of young animals, segments of adult retina were processed simultaneously to ensure the effectiveness of the technique. Furthermore, for control experiments, the anti-TH and anti-ChAT were replaced by either normal rabbit or rat serum or with PBS with the addition of 1% bovine serum albumen (antibody dilution) and then processed as above. Control retinas showed no positive immunoreactivity for TH or ChAT at any age examined. Retinas were laid receptorside down on a gelatinized slide and left to dry overnight at room temperature to ensure firm adhesion to the slide. They were then dehydrated in ascending alcohols, cleared in xylene, and mounted in Depex. Several retinas were counterstained with cresyl violet after completion of the immunocytochemistry to allow mapping of the ganglion cell distribution. Ganglion cells were identified by using the criteria set out by Stone ('78). For retinal sections, wholemounts were incubated as before, "sandwiched" between two pieces of filter paper, and dehydrated in ascending alcohols. They were then embedded flat in Histo-resin (LKB) and sectioned on a microtome at 10 μm .

Retinas were mapped systematically in 1-mm steps. Isodensity lines were traced by hand on translucent paper from the original maps and superimposed on a computer video screen. The isodensity lines were constructed by including values equal to or less than a criterion density inside the isodensity line. The area inside the isodensity line was then shaded to represent the density of the cells: the darker the shading, the higher the density (see Figs. 7, 8, 9, 12).

Dot maps and soma size analysis were undertaken with the Magellan program of Halasz and Martin ('84). For the dot maps in Figures 8 and 9, a horizontally elongated segment of retina chosen to include the area of peak ganglion cell density was scanned systematically in 120- μm steps, and a dot "placed" in the center of each immunoreactive soma encountered. For the soma size analysis, outlines of 50–100 adjacent immunoreactive somata were traced, and the system recorded the size of each soma as the diameter of a circle of equivalent area. Soma size analysis was also

- Blasdel, G., and D. Fitzpatrick (1984) Physiological organization of layer 4 in macaque striate cortex. *J. Neurosci.* 4:880-895.
- Colby, C.L., R. Gattass, C.R. Olson, and C.G. Gross (1988) Topographic organization of cortical afferents to extrastriate visual area PO in the macaque: A dual tracer study. *J. Comp. Neurol.* 269:392-413.
- Covey, E., R. Gattass, and C.G. Gross (1982) A new visual area in the parieto-occipital sulcus of the macaque. *Proc. Soc. Neurosci.* 8:681 (Abstract).
- Cowey, A. (1964) Projection of the retina on the striate and prestriate cortex in the squirrel monkey *Saimiri sciureus*. *J. Neurophysiol.* 27:366-393.
- Cragg, B.G. (1969) The topography of the afferent projections in the circumstriate cortex of the monkey studied by the Nauta method. *Vision Res.* 9:733-747.
- Cusick, C.G., H.J. Gould III., and J.H. Kaas (1984) Interhemispheric connections of visual cortex of owl monkeys (*Aotus trivirgatus*), marmosets (*Callithrix jacchus*), and Galagos (*Galago crassicaudatus*). *J. Comp. Neurol.* 230:311-336.
- Daniel, P.M., and D. Whitteridge (1961) The representation of the visual field on the cerebral cortex in monkeys. *J. Physiol. (Lond)* 159:203-221.
- De Yoe, E.A., S. Knierim, D. Sagi, B. Julesz, and D.C. Van Essen (1986) Single unit responses to static and dynamic texture patterns in macaque V2 and V1 cortex. *Invest. Ophthalmol. Vis. Sci.* 27(Suppl.):18 (Abstract).
- De Yoe, E.A., and D.C. Van Essen (1985) Segregation of efferent connections and receptive field properties in visual area V2 of the macaque. *Nature* 317:58-61.
- Fiorani, M., Jr. (1986) Topografia das Projeções Visuais na Área de Mielinização Densa da Parede Posterior do Sulco Temporal Superior (Área MT) no Macaco *Cebus apella*. MA Thesis, Instituto de Biofísica Carlos Chagas Filho, UFRJ, Rio de Janeiro.
- Gallyas, F. (1979) Silver staining of myelin by means of physical development. *Neurol. Res.* 1:203-209.
- Gattass, R., and C.G. Gross (1981) Visual topography of the striate projection zone in the posterior superior temporal sulcus (MT) of the macaque. *J. Neurophysiol.* 46:621-638.
- Gattass, R., C.G. Gross, and J.H. Sandell (1981) Visual topography of V2 in the macaque. *J. Comp. Neurol.* 201:519-539.
- Gattass, R., A.P.B. Sousa, and E. Covey (1986) Cortical visual areas of the macaque: Possible substrates for pattern recognition mechanisms. *Exp. Brain Res. (Suppl.)* 11:1-20.
- Gattass, R., A.P.B. Sousa, and M.G.P. Rosa (1984) Striate and extrastriate areas in the *Cebus* monkey: An electrophysiological and anatomical tracer study. *Proc. Soc. Neurosci.* 10:474 (Abstract).
- Gattass, R., A.P.B. Sousa, and M.G.P. Rosa (1987) Visual topography of V1 in the *Cebus* monkey. *J. Comp. Neurol.* 259:529-548.
- Gould, H.J. III, J.T. Weber, and R.W. Rieck (1987) Interhemispheric connections in the visual cortex of the squirrel monkey (*Saimiri sciureus*). *J. Comp. Neurol.* 256:14-28.
- Hoffstetter, R. (1982) Les primates Simiiformes (= Anthropeidea). (Comprehension, phylogénie, histoire biogéographique). *Ann. Paléont.* 68(3):241-290.
- Hubel, D.H., and M.S. Livingstone (1985) Complex-unoriented cells in a subregion of primate area 18. *Nature* 315:325-327.
- McIlwain, J.L. (1976) Large receptive fields and spatial transformation in the visual system. *Int. Rev. Physiol.* 10:223-248.
- Moran, J., R. Desimone, S.J. Schein, and M. Mishkin (1983) Suppression from ipsilateral visual field in area V4 of the macaque. *Proc. Soc. Neurosci.* 9:957 (Abstract).
- Piñon, M.C., A.P.B. Sousa, M.G.P. Rosa, and R. Gattass (1986) Aferentes corticais da área visual primária (V1) do macaco *Cebus*. *Proc. Braz. Soc. Neurosci.* 1:77 (Abstract).
- Rockland, K.S. (1985) A reticular pattern of intrinsic connections in primate area V2 (area 18). *J. Comp. Neurol.* 235:467-478.
- Rockland K.S., and D. Pandya (1981) Cortical connections of the occipital lobe in the rhesus monkey: Interconnections between areas 17, 18, 19, and the superior temporal sulcus. *Brain Res.* 212:249-270.
- Rosa, M.G.P., R. Gattass, and A.P.B. Sousa (1984) Split representation of the horizontal meridian in V2 in the *Cebus* monkey: A fluorescent tracer study. *Braz. J. Med. Biol. Res.* 17:410 (Abstract).
- Rosa, M.G., R. Gattass, and M. Fiorani, Jr. (1988) Complete pattern of ocular dominance stripes in V1 of a New World monkey, *Cebus apella*. *Exp. Brain Res.* (in press).
- Sanides, F. (1972) Representation in the cerebral cortex and its areal lamination patterns. In: G.H. Boune (ed): *Structure and Function of the Nervous System*. New York: Academic Press, pp. 329-453.
- Shipp, S., and S.M. Zeki (1985) Segregation of pathways leading from area V2 to areas V4 and V5 of the macaque monkey visual cortex. *Nature* 315:322-325.
- Spatz, W.B., and J. Tigges (1972) Species difference between Old World and New World monkeys in the organization of the striate-prestriate association. *Brain Res.* 43:591-594.
- Sousa, A.P.B., R. Gattass, M.C. Piñon, and M.G.P. Rosa (1987) Cortical afferents to striate cortex in the *Cebus* monkey. *Proc. Soc. Neurosci.* 13:625 (Abstract).
- Sousa, A.P.B., M.G.P. Rosa, and R. Gattass (1986) Anisotropic representation of the visual field in V1 and V2 in the *Cebus*. *Proc. Soc. Neurosci.* 12(2):1365 (Abstract).
- Tanaka, K., K. Hikosaka, H. Saito, M. Yukie, Y. Fukada, and E. Iwai (1986) Analysis of local and wide-field movements in the superior temporal visual areas of the macaque monkey. *J. Neurosci.* 6:134-144.
- Tigges, J., W.B. Spatz, and M. Tigges (1974) Efferent corticocortical fiber connections of area 18 in the squirrel monkey (*Saimiri*). *J. Comp. Neurol.* 158:219-235.
- Tootell, R.B.H., S.L. Hamilton, and M.S. Silverman (1985) Topography of cytochrome oxidase activity in owl monkey cortex. *J. Neurosci.* 5:2786-2800.
- Tootell, R.B.H., M.S. Silverman, R.L. De Valois, and G.H. Jacobs (1983) Functional organization of the second cortical visual area (V2) in the primate. *Science* 220:737-739.
- Tusa, R.J., A.C. Rosenquist, and L.A. Palmer (1979) Retinotopic organization of areas 18 and 19 in the cat. *J. Comp. Neurol.* 185:657-678.
- Van Essen, D.C., and J.H.R. Maunsell (1980) Two-dimensional maps of the cerebral cortex. *J. Comp. Neurol.* 191:255-281.
- Van Essen, D.C., W.T. Newsome, and J.L. Bixby (1982) The pattern of interhemispheric connections and its relationship to extrastriate visual areas in the macaque monkey. *J. Neurosci.* 2:265-283.
- Van Essen, D.C., W.T. Newsome, and J.H.R. Maunsell (1984) The visual field representation in striate cortex of the macaque monkey: Asymmetries, anisotropies and individual variability. *Vision Res.* 24:429-448.
- Van Essen, D.C., W.T. Newsome, J.H.R. Maunsell, and J.L. Bixby (1986) The projections from striate cortex (V1) to areas V2 and V3 in the macaque monkey: Asymmetries, areal boundaries and patchy connections. *J. Comp. Neurol.* 244:451-480.
- Van Essen, D.C., and S.M. Zeki (1978) The topographic organization of rhesus monkey prestriate cortex. *J. Physiol. (Lond.)* 277:193-266.
- Weller, R.E., and J.H. Kaas (1983) Retinotopic patterns of connections of area 17 with visual areas V-II and MT in macaque monkeys. *J. Comp. Neurol.* 220:253-279.
- Wong-Riley, M., and E.W. Carrol (1984) Quantitative light and electron microscopic analysis of cytochrome oxidase-rich zones in V-II prestriate cortex of the squirrel monkey. *J. Comp. Neurol.* 222:18-37.
- Zeki, S.M. (1969) Representation of central visual fields in prestriate cortex of the monkey. *Brain Res.* 14:271-291.
- Zeki, S.M., and D.R. Sandeman (1976) Combined anatomical and electrophysiological studies on the boundary between the second and third visual areas of rhesus monkey cortex. *Proc. R. Soc. Lond. [Biol.]* 194:555-562.